

1 **Antibodies from rabbits immunized with HIV-1 clade B SOSIP trimers can neutralize multiple**  
2 **clade B viruses by destabilizing the envelope glycoprotein**

3 MM van Haaren<sup>1</sup>, LE McCoy<sup>2,3</sup>, JL Torres<sup>4</sup>, W Lee<sup>4</sup>, CA Cottrell<sup>4</sup>, JL Copps<sup>4</sup>, P van der Woude<sup>1</sup>,  
4 A Yasmeeen<sup>5</sup>, SW de Taeye<sup>1</sup>, A Torrents de la Peña<sup>1</sup>, JP Moore<sup>5</sup>, DR Burton<sup>2,6,7</sup>, PJ Klasse<sup>5</sup>, AB  
5 Ward<sup>4,6,7</sup>, RW Sanders<sup>1,5</sup>¥, MJ van Gils<sup>1</sup>¥

6

7 <sup>1</sup>Department of Medical Microbiology, Amsterdam Infection & Immunity Institute, Amsterdam  
8 UMC, location AMC, University of Amsterdam, Amsterdam, 1105AZ, The Netherlands.

9 <sup>2</sup>Department of Immunology and Microbiology, The Scripps Research Institute, La Jolla, California,  
10 92037, USA.

11 <sup>3</sup>Division of Infection and Immunity, University College London, London, WC1E 6BT, UK.

12 <sup>4</sup>Department of Integrative Structural and Computational Biology, The Scripps Research Institute,  
13 La Jolla, California, 92037, USA.

14 <sup>5</sup>Department of Microbiology and Immunology, Weill Medical College of Cornell University, New  
15 York, New York, 10065, USA.

16 <sup>6</sup>International AIDS Vaccine Initiative - Neutralizing Antibody Center (IAVI-NAC), The Scripps  
17 Research Institute, La Jolla, CA 92037, USA.

18 <sup>7</sup>Center for HIV/AIDS Vaccine Development (CHAVD), The Scripps Research Institute, La Jolla, CA  
19 92037, USA.

20

21 **¥ Corresponding authors:**

22 Rogier W. Sanders, PhD; R.W.Sanders@amsterdamumc.nl

23 Marit J. van Gils, PhD; M.J.vangils@amsterdamumc.nl

24 **ABSTRACT**

25           The high HIV-1 viral diversity is a formidable hurdle for the development of an HIV-1  
26 vaccine. Elicitation of broadly neutralizing antibodies (bNAbs) would offer a solution, but so  
27 far immunization strategies have failed to elicit bNAbs efficiently. To overcome the obstacles,  
28 it is important to understand the immune responses elicited by current HIV-1 envelope  
29 glycoprotein (Env) immunogens. To gain more insight, we characterized monoclonal  
30 antibodies (mAbs) isolated from rabbits immunized with Env SOSIP trimers based on the clade  
31 B isolate AMC008. Four rabbits that were immunized three times with AMC008 trimer  
32 developed robust autologous and sporadic low-titer heterologous neutralizing responses.  
33 Seventeen AMC008 trimer-reactive mAbs were isolated using antigen-specific single B cell  
34 sorting. Four of these mAbs neutralized the autologous AMC008 virus and several other clade  
35 B viruses. When visualized by electron microscopy, the complex of the neutralizing mAbs with  
36 the AMC008 trimer showed binding to the gp41 subunit with unusual approach angles and we  
37 observed that their neutralization ability depended on their capacity to induce Env trimer  
38 dissociation. Thus, AMC008 SOSIP trimer immunization induced clade B neutralizing mAbs  
39 with unusual approach angles with neutralizing effects that involve trimer destabilization.  
40 Optimizing these responses might provide an avenue to the induction of trimer dissociating  
41 bNAbs.

42

43 **Keywords**

44 HIV-1, vaccine, monoclonal antibodies, AMC008 SOSIP, trimer destabilization, approach angle

45

46 **IMPORTANCE**

47           Roughly 32 million people have died as a consequence of HIV-1 infection since the start  
48 of the epidemic and still 1.7 million people get infected with HIV-1 annually. Therefore, a  
49 vaccine to prevent HIV-1 infection is urgently needed. Current HIV-1 immunogens are not able  
50 to elicit the broad immune responses needed to provide protection against the large variation  
51 of HIV-1 strains circulating globally. A better understanding of the humoral immune responses  
52 elicited by immunization with state-of-the-art HIV-1 immunogens should facilitate the design  
53 of improved HIV-1 vaccine candidates. We identified antibodies with the ability to neutralize  
54 multiple HIV-1 viruses by destabilization of the envelope glycoprotein. Their weak but  
55 consistent cross-neutralization ability indicates the potential of this epitope to elicit broad  
56 responses. The trimer-destabilizing effect of the neutralizing mAbs combined with detailed  
57 characterization of the neutralization epitope can be used to shape the next generation of  
58 HIV-1 immunogens to elicit improved humoral responses after vaccination.  
59

## 60 INTRODUCTION

61 The ongoing HIV-1 epidemic, in spite of effective HIV-1 medication, highlights the need  
62 for an HIV-1 vaccine. To achieve this goal, knowledge on the immune responses elicited by  
63 state-of-the-art HIV-1 immunogens is important. Such knowledge will allow the further  
64 optimization and development of these immunogens. Many immunogens that are being  
65 explored as subunit vaccines are based on the HIV-1 envelope glycoprotein (Env) trimer (1–6).  
66 The Env trimer is the only viral protein expressed on the outside of the HIV-1 particle and  
67 therefore the only target for neutralizing antibodies (NAbs). Because circulating HIV-1 viruses  
68 have extremely diverse Env sequences, in order to provide protection, an HIV-1 vaccine needs  
69 to induce broadly NAbs (bNAbs), i.e. NAbs that can cope with Env diversity(7). Extensive  
70 research has provided the field with soluble, stable, and native-like versions of Env, including  
71 SOSIP trimers(8). So far, SOSIP trimers have generally elicited strong autologous NAb  
72 responses, but only sporadic, inconsistent, and weak cross-NAb responses(9–12). It is  
73 imperative to study these Ab responses to understand precisely which improvements are  
74 needed to consistently broaden the response. Iterative vaccine design based on monoclonal  
75 Abs (mAbs) isolated from vaccinated animals is a valuable way to overcome the limitations of  
76 the current HIV-1 immunogens(13, 14).

77 Previous studies characterizing mAbs and bulk serum of SOSIP Env trimer immunized  
78 rabbits and macaques showed that the Ab responses frequently target strain-specific glycan  
79 holes(15–17). Indeed, the immunodominance of glycan holes was confirmed by re-direction  
80 of vaccine induced Ab responses towards *de novo* glycan holes when the original strain-  
81 specific glycan hole was filled(18). Env trimers from different virus isolates probably have their  
82 own specific immunodominant glycan holes, which would explain why Env-trimer immunized

83 animals develop very limited neutralization breadth. Another immunodominant region after  
84 immunization is the unprotected base of the soluble Env trimer (17, 19, 20). This region of the  
85 Env trimer is, in its natural display, concealed by the viral membrane and in no need of heavy  
86 glycosylation to evade the immune system. However, on soluble Env trimers the base forms a  
87 large glycan hole that is easily accessed by the immune system, and induces Abs that cannot  
88 recognize the full length Env trimer, i.e. are non-NAbs.

89 Many vaccine induced NAbs target epitopes that overlap those of non-NAbs(11, 15,  
90 16). Yet, it is unclear what exactly determines whether an Ab will have neutralizing ability. For  
91 some Ab families binding kinetics might influence neutralization ability(21, 22). Indeed, it was  
92 shown that some Ab families elicited during natural infection have kinetics of Ab binding that  
93 correlate with their neutralization ability. In particular a high off-rate constant was associated  
94 with absent or less effective neutralization. The on-rate constant and overall affinity appeared  
95 to be of less influence on the ability to neutralize(21, 22).

96 SOSIP-induced NAbs have been discovered that target the same epitope as well-known  
97 bNAbs elicited after natural HIV-1 infection, but without displaying the same potency or  
98 breadth(17, 19, 23–25). Some studies have shown that the approach angle is relevant in this  
99 respect. For instance, for CD4-binding site (CD4-bs) directed Abs the correct approach angle  
100 is essential for their ability to neutralize. The right approach angle allows bNAbs to reach the  
101 CD4bs while circumventing the dense Env glycan shield(23).

102 Several vaccines involving state-of-the-art Env trimer immunogens(1, 10) or specific  
103 Env epitope scaffolds(26, 27) have induced sporadic NAb responses against heterologous  
104 viruses in addition to autologous NAbs. Although such heterologous neutralization can be  
105 broad, spanning many clades, it is usually not very potent. Interestingly, two bNAbs have been

106 isolated from a rabbit immunized with Env trimers on liposomes(1). The serum of this rabbit  
107 serum exhibited broad neutralization, and the isolated bNAbs recapitulated that activity. The  
108 development of breadth in this one rabbit was exceptional, as none of the other rabbits  
109 receiving the same immunogens developed this remarkable neutralization breadth, but the  
110 detailed characterization of such immune responses through the isolation of mAbs helps to  
111 understand why the development of neutralization breadth is rare, and how it can be  
112 improved.

113 In this study we isolated mAbs from four rabbits immunized with the clade B Env trimer  
114 immunogen AMC008 SOSIP. We identified an immunodominant area on the gp41 subunit of  
115 the AMC008 SOSIP trimer. Interestingly, these NAbs could cross-neutralize other clade B  
116 viruses. Negative-stain electron microscopy (NS-EM) revealed that these NAbs bound with an  
117 unusual approach angle that would be expected to be incompatible with binding to virus-  
118 associated Env trimers because of a clash with the viral membrane. Contrary to expectations  
119 and despite the unusual angle of approach, these mAbs were able to bind and neutralize,  
120 demonstrating remarkable flexibility of virus-associated Env trimers in their interaction with  
121 Abs(28). We further showed that the neutralization capacity of these NAbs depended on their  
122 ability to dissociate the Env trimer, similarly to what has been described previously for bNAbs  
123 isolated from both humans and rabbits(1, 29). The information gathered from this study helps  
124 to elucidate mechanistic aspects of virus neutralization and may help to tailor immunogens to  
125 elicit trimer dissociating NAbs.

126

## 127 **RESULTS**

128 *AMC008 SOSIP immunization induces NAbs and non-NAbs*

129 In a previous study by our group, fifteen rabbits (animal IDs: 1594-1608) were  
130 immunized with the clade B Env trimer AMC008 SOSIP(10). This immunogen was based on the  
131 viral sequence from an individual enrolled in the Amsterdam Cohort Studies (ACS) that  
132 showed broad serum neutralization(10). All AMC008 SOSIP trimer-immunized rabbits showed  
133 consistent autologous neutralization as well as low cross-neutralization of the clade B viruses  
134 BaL, REJO, WITO, and SHIV162p3(10). We further investigated serum neutralization of animals  
135 1605-1608 and observed cross-neutralized at low titers by two and four rabbits of the clade B  
136 viruses AMC009 and AMC018, isolated from different HIV-infected individuals (**figure 1A**). To  
137 better understand the cross-neutralization in these animals and its limitations, mAbs were  
138 isolated from these four AMC008 SOSIP trimer-immunized rabbits. PBMCs were obtained  
139 from these animals at week 21, one week after the third immunization (**figure 1A**). Single B  
140 cells expressing IgG, and with the ability to bind two distinctly labeled, fluorescent AMC008  
141 SOSIP trimers were selected by fluorescence-activated cell sorting (FACS). On average, 5% of  
142 total live B cells were AMC008 SOSIP trimer-reactive. B cell receptor (BCR) sequences were  
143 subsequently amplified and cloned into expression vectors to generate mAbs that were tested  
144 for binding to autologous AMC008 SOSIP trimers in ELISA. A total of 17 mAbs bound the  
145 AMC008 SOSIP trimer. Rabbits 1605 and 1607 yielded 7 and 8 mAbs respectively, while from  
146 the other two rabbits (1606 and 1608) only one mAb each was generated (**figure 1B**).

147 Sequence analysis of the heavy chain variable region showed the expected polyclonal  
148 immune response within each rabbit (**figure 1C**). From these sequences we determined the  
149 length of the complementary determining region 3 of heavy and light chains (CDRH3 and  
150 CDRL3, respectively). The CDRH3 is important as it interacts directly with the immunogen and  
151 is often elongated in human bNAbs to cope with the extensive glycan shield surrounding the

152 Env trimer(30, 31). We also analyzed the CDRL3 because rabbit Abs, in contrast to human Abs,  
153 usually interact with the immunogen predominantly through the CDRs of their light chain(32).  
154 The average length of the CDRH3 of all AMC008 SOSIP trimer-reactive mAbs was 15 amino  
155 acids, which agrees with previous studies on CDRH3 lengths of BCR sequences in naïve  
156 rabbits(32, 33) (**figure 1D**). However, the individual CDRH3 length varied greatly, ranging from  
157 10-22 amino acids. The average CDRL3 length was increased with 2 amino-acid residues to an  
158 average of 14 residues in AMC008 SOSIP trimer-reactive mAbs from 12 residues in BCR  
159 sequences from naïve rabbits(32, 33). The distribution of the individual CDRL3 lengths in the  
160 rabbits was more limited than that of the CDRH3 region, ranging from 11-16 amino acids  
161 (**figure 1D**).

162 We then tested the isolated mAbs for their ability to neutralize the autologous AMC008  
163 virus (**figure 1E**). Four of the seventeen mAbs were able to neutralize the AMC008 virus  
164 although with relatively low potency ( $IC_{50}$  values ranging from 16-19  $\mu\text{g}/\text{mL}$ ). Three of the  
165 identified four NAbS were isolated from rabbit 1605 and belonged to the same clonal family;  
166 these were designated 05A1, 05A2, and 05A3. The fourth NAb was isolated from rabbit 1607  
167 and named 07A1. Alignment of heavy and light chain variable regions revealed 93% sequence  
168 similarity between the CDRL3 sequences of the 05A family (**figure 1C**). In addition, we found  
169 no evidence of gene conversion, a common feature for rabbit antibodies, within this family of  
170 3 mAbs. Interestingly, NAb 07A1 CDRL3 region similar to that of 05A1-3 (79% sequence  
171 similarity). This shared CDRL3 was relatively long with a length of 14 amino acids. The heavy  
172 chain CDR sequences of the 05A family and 07A1 did not show any similarities (**figure 1C**).

173

174 *AMC008 SOSIP-induced NAbS cross-neutralize some clade B viruses*

175           The cross-binding ability of the NAbS was tested against a panel of 12 heterologous  
176 SOSIP Env trimers (**table 1**). This panel included four clade B SOSIP Env trimers (AMC009,  
177 AMC011, AMC016, and AMC018) based on virus sequences from individuals enrolled in the  
178 ACS(34). The Env sequences from these four clade B SOSIP trimers have >83% sequence  
179 identity with the AMC008 Env protein. Additional Clade B SOSIP Env trimers derived from  
180 SHIV162p3 and REJO, 79% and 84% sequence identity with AMC008 respectively, were also  
181 included in the panel, as neutralization of these viruses by the corresponding rabbit sera was  
182 observed previously (10). Furthermore, we included a selection of non-clade B SOSIP trimers  
183 from a representative global panel i.e. CNE55 (clade CRF01\_AE), BJOX002000.03.2 (clade  
184 CRF07\_BC), Ce1176\_A3 (clade C), 25710-2.43 (clade C)(35), as well as BG505 (clade A)(5) and  
185 finally the ConM SOSIP trimer, a consensus sequence protein based on the consensus  
186 sequences of each individual HIV-1 Group M clade(36). All four NAbS displayed cross-reactivity  
187 with five out of the six clade B SOSIP Env trimers (**table 1**). The NAb family 05A1-A3 also bound  
188 to the clade C SOSIP trimer Ce1176\_A3 but there was no binding to other SOSIP trimers,  
189 suggesting that the target epitope is fairly conserved in clade B isolates but not across different  
190 clades.

191           All four NAbS were then tested for neutralization breadth against a panel of 17  
192 heterologous viruses consisting of a subpanel representing the global diversity of HIV-1  
193 supplemented with a number of clade B viruses(35). Two of the viruses in this heterologous  
194 panel, the clade B tier 2 viruses SHIV162p3 and AMC009, were cross-neutralized by all four  
195 NAbS (**table 2**). SHIV162p3 was neutralized relatively weak with IC<sub>50</sub> values ranging from 5.6-  
196 19 µg/mL, i.e. similar to those against the autologous AMC008 virus. Heterologous AMC009  
197 neutralization by the NAbS was much weaker, with IC<sub>50</sub> values ranging from 58-177 µg/mL.

198 The relative cross-neutralization of autologous AMC008 and heterologous SHIV162p3 and  
199 AMC009 is consistent with the cross-neutralization titers of the serum of the rabbits 1605 and  
200 1607(10).

201

202 *AMC008 NAbs target an epitope on the gp41 subunit*

203 Because the four NAbs had nearly identical CDRL3 sequences and three of them were  
204 clonal family members, we hypothesized that they might target a shared epitope. To test this,  
205 we performed competition assays between these four NAbs using Bio-layer interferometry  
206 (BLI). All NAbs showed strong and reciprocal competition with each other, suggesting that  
207 their epitopes overlap (**figure 2A**). Differences in percentage of residual binding were  
208 observed depending on the directionality of the assay. For instance, we observed 54% residual  
209 binding of 05A2 after pre-incubation with competitor 07A1 mAb. However, only 9% residual  
210 binding of 07A1 was measured when 05A2 was used as the competitor. These differences  
211 could be due to differences in affinity of the NAbs. All mAbs showed self-competition (46-27%  
212 residual binding) (**figure 2A**).

213 We then performed competition assays with known human bNAbs using ELISA and  
214 Surface Plasmon Resonance (SPR) to specify the epitope targeted by these four NAbs. We  
215 tested competition with bNAbs VRC01, PGT121, 35O22, 3BC315, PGT151, and ACS202. These  
216 bNAbs target diverse regions on the Env trimer enabling us to define a potential binding area  
217 of NAbs 05A1-A3 and 07A1. All four NAbs competed significantly in ELISA with bNAbs 35O22,  
218 3BC315, and VRC34 which all target gp41. Competition of the four NAbs 05A1, 05A2, 05A3  
219 and 07A1 with 35O22 was weakest with residual binding being 58%, 69%, 73%, and 67%,  
220 respectively (**figure 2B**). The four NAbs competed more efficiently with VRC34 and 3BC315

221 with residual binding between 25% and 60% (**figure 2B**). Weak but not statistically significant  
222 competition was observed with gp41-gp120 targeting bNAb ACS202 and no statistically  
223 significant competition was detected with gp41-gp120 targeting bNAb PGT151, or bNAb  
224 VRC01 or PGT121, which bind to the CD4bs and the V3-N332 glycan epitope, respectively.

225 SPR analyses strengthened the evidence for competition of the 05A family with gp41-  
226 gp120-targeting bNAb 35O22 (~25% residual binding) and ACS202 (~60% residual binding),  
227 and also revealed weak competition with PGT151 (~80% residual binding) (**figure 2B**). The  
228 competition with ACS202 was enhanced when the SPR assay set-up was reversed. In this  
229 reversed set-up, where ACS202 was allowed to bind first and 05A1-3 second, the residual  
230 binding dropped to ~10% (**figure 2C**). No significant competition of the rabbit NAb with the  
231 bNAb VRC01 and PGT121 was observed in the SPR assays in both set-ups (**figure 2B**). These  
232 competition results suggest that the AMC008 SOSIP induced NAb that most likely target an  
233 epitope at or near the gp41-gp120 interface area.

234 We also tested competition of the AMC008 SOSIP trimer induced NAb with the non-  
235 NAb elicited against the same immunogen using bio-layer interferometry (BLI). The binding  
236 of the four NAb to the AMC008 SOSIP trimers was completely or partially abrogated when  
237 either of the five non-NAb 06A1, 07B1, 07D2, 07E1, or 08A1 was present. These competition  
238 results suggest that these five non-NAb have overlapping epitopes with the NAb (**figure 2D**).  
239 The remaining five non-NAb did not compete with the NAb, suggesting these target different  
240 epitopes on the Env trimer.

241 Negative stain electron microscopy (NS-EM) was performed to further delineate the  
242 NAb epitope and to confirm its location at or near the gp41-gp120 interface. Binding of Fab  
243 fragments from the four identified NAb to the AMC008 SOSIP trimer was visualized through

244 3D reconstructions. The NAb Fabs interacted with the gp41 subunit of the AMC008 SOSIP  
245 trimer, possibly interacting with residues S528-A532, N616-N625, and Q658-D644 in the HR2  
246 region (**figure 3A**). Additional NS-EM analysis carried out with 05A3 revealed that it bound  
247 with a predominant stoichiometry of two Fabs to one Env trimer, although full occupancy of  
248 three Fabs binding to one trimer could be detected in a minority of cases. Interestingly, the  
249 NAb interacted with the Env trimer with unusual approach angles that would *a priori* be  
250 expected to lead to a clash of the NAb with the viral membrane.

251

252 *AMC008 NAb target residues 620 and 624 in HR2*

253 The NS-EM analysis enabled us to make informed changes to identify amino-acid  
254 residues important for binding and neutralization. Within predicted interaction regions  
255 pinpointed by the NS-EM analysis, we searched for differences between the sequences of Env  
256 trimers that the NAb were able to cross-bind and/or neutralize, and those that they could  
257 not bind or neutralize (**figure 3B**). Divergent amino acids were mutated in the context of  
258 AMC008 SOSIP trimer and corresponding pseudovirus to the most prevalent amino acid in the  
259 non-binding sequences, resulting in three variants with single amino acid substitutions, i.e.,  
260 D620N, N624D, and E662A. In addition, considering that Env glycans might influence NAb  
261 binding, we modified the glycan shield near or on gp41 of the AMC008 trimer. Accordingly,  
262 knock-out (KO) mutants of the potential N-linked glycosylation sites (PNGS) at position 88,  
263 611, 616, and 637 were created. Finally, since previous studies showed that SOSIP-induced  
264 NAb often target strain specific holes in the glycan shield(15–17, 25), we knocked-in (KI) the  
265 PNGS at positions 230 and 234 of the AMC008 sequence, as the absence of PNGS at these  
266 positions in the natural AMC008 sequence is expected to create a strain-specific glycan hole

267 (figure 3C). Substitution of amino acids 620 and 624 abolished neutralization ability of all four  
268 NABs, but not of the control Ab VRC01, consistent with the NS-EM data (figure 3D and 3E).  
269 Furthermore, neutralization by 07A1 was also affected by introducing simultaneously the  
270 N230 and N234 PNGS, although these substitutions did not completely abrogate activity, as  
271 neutralization of the virus still occurred at higher Ab concentrations. This suggests that glycans  
272 at N230 and N234 restrict access to the 07A1 epitope. Three out of four NABs were also  
273 affected by removing the N611 and N637 PNGS: these glycans might therefore contribute to  
274 (the presentation of) the NAB epitope. The K232T and K236T single KI mutations did not affect  
275 neutralization for any of the four NABs and neither did the N88, and N616 KO mutations, or  
276 the E662A amino acid substitution. When residues 230, 234, 611, 620, 624, or 637 were  
277 mutated in the AMC008 SOSIP trimer context, it did not detectably affect binding of NABs  
278 05A1-A3 in ELISA, while the effect on NAb 07A1 was only observed when residues 620 and  
279 624 were changed (figure 4A). Differential effects of single mutations in neutralization versus  
280 binding assays have been observed in other cases(37, 38), and probably relate to affinity and  
281 Env protein conformation and stability.

282 We were also able to define the epitopes for the majority of the non-NABs. mAbs 07E1  
283 and 07D2 also showed dependence on the 620, 624, and/or 662 amino acids in ELISA (Figure  
284 4A), confirming their epitope overlap with the NABs as suggested by the competition  
285 experiments. NS-EM further confirmed this epitope overlap for non-NAB 07D2 (figure 4B).  
286 Other non-NABs bound a variety of epitopes on the gp41 subunit of the Env trimer such as the  
287 area around the N637 glycan (07F1) (Figure 4A), and an epitope at the base of the Env trimer  
288 (07B1). The non-NAB 05D1 was able to bind a linear V3 peptide in ELISA (Figure 4A).  
289

290 *NAbs and non-NAbs targeting the 620/624 site cannot be differentiated based on affinity for*  
291 *soluble trimer*

292 We were intrigued by the identification of NAb and non-NAb that targeted  
293 overlapping epitopes. A first hypothesis would be that binding affinity might explain the  
294 differences in neutralization ability between NAb and non-NAb. To test this, we subjected a  
295 subset of AMC008 SOSIP-induced non-NAb and all four NAb, to kinetic binding experiments  
296 with AMC008 SOSIP Env trimers. No significant differences were observed in affinity between  
297 the NAb and the non-NAb ( $P = 0.057$  for  $K_D$ ,  $P = 0.057$  for  $K_a$  and  $P > 0.999$  for  $K_d$ ; Mann-  
298 Whitney U test) (**figure 5A**).

299 We also noted that all four NAb were able to cross-bind certain SOSIP Env trimers, but  
300 were unable to neutralize their corresponding virus. We asked whether this observation could  
301 be explained by differences in affinity as well. We tested all four of the NAb in kinetic binding  
302 experiments using AMC008 SOSIP and AMC016 SOSIP Env trimers. The latter was selected in  
303 addition to the autologous trimer because the AMC016 virus was not neutralized by our NAb,  
304 while they were able to bind to the corresponding AMC016 SOSIP trimer (**table 2**). AMC016  
305 SOSIP trimers contain the amino acids essential for neutralization (D620 and N624) but also  
306 the N230 and N234 PNGS that are absent from the AMC008 Env sequence. Kinetic analysis did  
307 not reveal significant differences in NAb binding kinetics between the AMC008 SOSIP and  
308 AMC016 Env trimers ( $P = 0.343$  for  $K_D$ ,  $P = 0.114$  for  $K_a$  and  $P = 0.486$  for  $K_d$ ; Mann-Whitney  
309 U test) (**figure 5A**), suggesting that binding kinetics are not the main cause for the (in)ability  
310 of these NAb to neutralize these viruses.

311

312 *NAbs and non-NAbs targeting the 620/624 site cannot be differentiated based on binding to*  
313 *membrane associated Env trimer*

314         The next hypothesis posits that the discrepancy between binding and neutralization  
315 ability of the autologous AMC008 SOSIP Env trimer-reactive mAbs might be due to an inability  
316 of the non-NAbs to bind full length-surface displayed Env trimers, possibly related to the  
317 observed unusual approach angle. To test this, we transfected HEK293 cells with AMC008  
318 SOSIP gp160 Env constructs(39), which resulted in surface expressed AMC008 SOSIP trimers,  
319 that were subsequently analyzed by FACS to detect mAb binding (**figure 5B**). In contrast to  
320 what we expected, we found that NAbs and non-NAbs bound similarly to full-length, cell-  
321 surface-displayed AMC008 SOSIP gp160 trimers. Surprisingly, we found that the NAb 05A3  
322 bound weakly, and NAb 07A1 was unable to bind cell-surface-displayed SOSIP gp160 trimers,  
323 which is somewhat inconsistent with their ability to neutralize.

324

325 *Neutralization activity of mAbs against the 620/624 epitope is determined by their ability to*  
326 *disrupt the trimer*

327         A third hypothesis argues that the strength of neutralization is strongly influenced by  
328 the capability to induce trimer dissociation. Indeed, gp41 targeting human bNAbs 3BC315 and  
329 3BC176 neutralize by inducing dissociation of the Env trimer and so does rabbit bNAbs 1C2  
330 derived from an immunization study(1, 29). We noticed that the 05A3 fab fragments caused  
331 the trimer to dissociate into monomers during sample preparation for NS-EM (**figure 6A**).  
332 Dissociation of the AMC008 SOSIP Env trimer did not occur spontaneously when the trimer  
333 was left overnight at RT in the absence of 05A1 or 05A3, suggesting that the fab was  
334 responsible for the observed trimer dissociation.

335 To corroborate these findings, we performed a neutralization assay with prolonged  
336 pre-incubation times (29). This assay determines the neutralization ability of an Ab after pre-  
337 incubation over a 24-hour time at 37 °C period to measure irreversible trimer destabilization.  
338 An increase of neutralization with longer incubation times is indicative of trimer  
339 destabilization as more trimers are destabilized by the Ab over time(1, 29). The bNABs PGT126  
340 and 3BC315 were tested in this assay as negative and positive controls, respectively, and  
341 showed an increase in neutralization potency of 1.5-fold and 10-fold, respectively, after 24 vs  
342 1 hour incubation. The potency of our NABs against the autologous AMC008 virus increased  
343 by ~10-fold after 24 hours incubation (**figure 6B**), indicative of trimer dissociation and similar  
344 to the effect of 3BC315. The non-NAB 6A1, targeting a similar epitope as our NABs, remained  
345 unable to neutralize the AMC008 virus even after 24 hours of incubation. The results were  
346 even more pronounced with the heterologous SHIV162p3 virus, showing increases in potency  
347 of up to nearly 30-fold after 24 hours. Interestingly, the NAb 05A1 did show an increase in  
348 potency against the AMC008 virus over time, but no significant increase against the  
349 heterologous SHIV162p3 virus. Nevertheless, these data indicate that the four NABs dissociate  
350 Env trimers of both autologous and heterologous viruses and that this largely contributed to  
351 their neutralization capacity.

352

### 353 **DISCUSSION**

354 To overcome viral diversity an HIV-1 vaccine should induce bNABs. However, the  
355 currently used immunogens have been unable to consistently elicit such responses. In this  
356 study we tried to better understand the humoral immune responses after HIV-1 SOSIP Env  
357 trimer immunization in rabbits. We set out to determine which epitopes on the clade B

358 AMC008 SOSIP Env trimer were targeted, and whether the observed specificities could explain  
359 the low-titer heterologous neutralization that was observed after immunization with this  
360 SOSIP trimer. We isolated and characterized 17 mAbs from four AMC008 SOSIP Env trimer-  
361 immunized rabbits. The vast majority of the isolated mAbs targeted a similar area in the HR2  
362 region. One antibody family (05A) and the mAb 07A1 were found to neutralize the autologous  
363 and two heterologous viruses through destabilization of the Env trimer. A mechanism of  
364 neutralization also used by NAbs induced by natural infection or vaccination(1, 29).  
365 Additionally, we identified important contact residues for these NAbs. Such knowledge may  
366 help to shape next generation SOSIP Env trimer immunogens to induce trimer destabilizing  
367 NAbs.

368         Even though rabbits are a widely used animal model in the early stages of HIV-1 vaccine  
369 testing, we realize there are caveats to using this model. In contrast to humans, rabbits  
370 interact with the antigen predominantly through their light chain(32) and use one heavy V-  
371 gene in the initial Ab recombination process, therefore, diversity in the heavy chain is much  
372 more restricted compared to their light chains. Additionally, gene conversion and somatic  
373 hypermutation (SHM) are the major drivers of Ab diversity in rabbits, the former is a process  
374 that rarely takes place in humans(32, 40). Nonetheless, numerous isolated rabbit Abs show  
375 that similar epitopes on the Env trimer are targeted as seen in macaques and humans after  
376 natural infection(41).

377         Although the NAbs that we describe do not have the desired breadth for a protective  
378 HIV-1 vaccine, they are rare examples of mAbs with consistent, albeit weak, cross-neutralizing  
379 ability, in particular after only three immunizations with only one immunogen. Other  
380 experiments have yielded only autologous neutralizing mAbs with the notable exception of

381 the isolation of two bNAbs from one Env-immunized rabbit(1, 16, 19, 25). Valuable  
382 information from these previous studies led to the development of new immunogens, such as  
383 Env trimers displayed on nanoparticles, germline trimers, and specific epitope scaffolds that  
384 were expected to induce more broad and consistent neutralization (2, 27, 42, 43).  
385 Nonetheless, neutralization breadth in rabbits after HIV-1 immunization remains sporadic and  
386 usually of low titer(9–12). The isolation of heterologous NABs from multiple rabbits using the  
387 same neutralization mechanism and targeting similar epitopes highlights the possibility for  
388 immune focusing towards this epitope cluster. The identification of bNAbs isolated from both  
389 humans and rabbits targeting similar epitopes, with the shared capacity to disrupt trimers,  
390 marks this epitope as a very interesting target to be further exploited(1, 29).

391         bNAb 1C2 that exhibited an extraordinary broad NAb response (~85%) was isolated  
392 from an Env-immunized rabbit(1). The mechanism of 1C2 neutralization involved  
393 destabilization of the Env trimer similar to the effects of bNAbs 3BC315 and 3BC176(29), and  
394 NAb family 05A and 07A1 described here. It was proposed that these bNAbs destabilize the  
395 trimer by disruption of the stabilizing tryptophan clasp formed by amino acids W623, W628,  
396 and W631(1, 44). The CDRH3 loops of both rabbit bNAb 1C2 and human bNAb 3BC315 are  
397 close to residue W623 of this clasp. Because the NABs we describe here have contacts with  
398 residues 620 and 624, neighboring this tryptophan clasp, it is not unlikely that a similar  
399 disruption mechanisms is utilized by these rabbit NABs. The description of multiple (b)NABs  
400 directed to this epitope, with the same potent mechanism of action would indicate this  
401 epitope as a potential vaccine target. Nonetheless, the isolation of both bNAbs, NABs, and  
402 non-NABs directed to this epitope shows that adaptations to the immunogen are necessary  
403 to amplify this desirable response and guide the responses to neutralization potency and

404 breadth. One strategy involves glycan modifications to enhance accessibility of the tryptophan  
405 clasp. Another complementary strategy could involve immune focusing on conserved amino  
406 acids within this region as opposed to ones that are more variable such as residues 620 and  
407 624.

408         The AMC008 SOSIP Env trimer lacks the N230 and N234 PNGS, generating a strain-  
409 specific glycan hole. The absence of these glycans might dictate the angle of approach for the  
410 NAbS identified in this study, and thereby restrict the breadth of the response. Filling the  
411 230/234 glycan hole negatively impacted neutralization by the NAb 07A1. However, this was  
412 not the case for the NAbS isolated from animal 1605. One explanation might be that the  
413 footprint of the 07A1 epitope is larger and/or in closer proximity to the 230/234 glycan hole.  
414 The ability of these NAbS to neutralize viruses containing the 230 and 234 PNGS, such as the  
415 SHIV162p3 virus, is encouraging as the 234 PNGS is widely conserved.

416         The NS-EM revealed an improbable approach angle for the NAbS that should result in  
417 a clash with the viral membrane. Possibly the angles by which the NAbS approach soluble Env  
418 trimers and virus-associated Env might vary, in particular at the trimer stem. For instance, the  
419 MPER bNAb 10E8 Fab approaches soluble SOSIP trimers with an angle similar to that of 05A1-  
420 A3 and 07A1, but this angle changes to facilitate the presence of the membrane when 10E8  
421 binds to membrane-anchored Env(45). Moreover, viral membrane-associated envelope  
422 proteins can have remarkable flexibility. This flexibility was visualized for the SARS-CoV-2 spike  
423 protein which is able to tilt by up to  $\sim 60^\circ$  relative to a position perpendicular to the  
424 membrane(46). Also, HIV-1 Env trimers on nanodiscs displayed the ability to tilt by  $\sim 20^\circ$  when  
425 bound to gp41 directed bNAbS(28).

426 Previous studies suggested that a slower dissociation was associated with stronger  
427 neutralization(21, 22). However, this did not apply to the gp41-directed mAbs described here.  
428 One difference is that these mAbs originated from different clonal families, whereas the  
429 previous studies analyzed clonal family members. Furthermore, we determined binding  
430 kinetics using stabilized soluble Env SOSIP trimers. It cannot be excluded that Env stabilization  
431 in the SOSIP construct and the observed destabilization of the Env trimer by the Nabs might  
432 have affected the affinities we measured. Nevertheless, it is likely that a slow dissociation and  
433 the ability to induce trimer dissociation are distinct properties that affect both neutralization  
434 potency and efficacy(47).

435 In summary, characterizing humoral immune responses at the mAb level after  
436 immunization can inform future immunization studies and strategies. We found that gp41-  
437 directed NAbs with an unusual approach angle, predicted to clash with the viral membrane,  
438 were able to weakly neutralize autologous and heterologous clade B viruses by inducing Env  
439 trimer destabilization, reminiscent of bNAbs that induce trimer dissociation by disrupting the  
440 tryptophan clasp in gp41. This knowledge highlights that destabilization of the trimer might  
441 be a more important neutralization mechanism than previously appreciated. Inducing trimer  
442 destabilizing NAbs that target the tryptophan clasp should be considered in future  
443 immunization strategies.

444

#### 445 **Acknowledgements**

446 This work was supported by the HIV Vaccine Research and Design (HIVRAD) program (P01  
447 AI110657) (to A.B.W., J.P.M., P.J.K., and R.W.S), the Bill and Melinda Gates Foundation  
448 through the Collaboration for AIDS Vaccine Discovery (CAVD), grants OPP1111923,

449 OPP1132237 and INV-002022 (to R.W.S.), and grant OPP1170236 (to A.B.W.); by the European  
450 Union's Horizon 2020 research and innovation program under grant agreement No. 681137  
451 (to R.W.S); by NIH under grant number AI36082 (to J.P.M. and P.J.K.). Support was also  
452 obtained from an equipment grant from the Fondation Dormeur, Vaduz (to R.W.S. and M.J.G.).  
453 R.W.S. is a recipient of a Vici grant from the Netherlands Organization for Scientific Research  
454 (NWO). M.J.G. is a recipient of an AMC Fellowship and a Mathilde Krim Fellowship from the  
455 American Foundation for AIDS Research (amfAR) (109514-61-RKVA). The electron microscopy  
456 data were collected at Electron Microscopy Facility of the Scripps Research Institute. The  
457 Amsterdam Cohort Studies (ACS) on HIV infection and AIDS, a collaboration between the  
458 Amsterdam Health Service, the Academic Medical Center of the University of Amsterdam,  
459 Sanquin Blood Supply Foundation, and the Jan van Goyen Clinic, are part of The Netherlands  
460 HIV Monitoring Foundation and are financially supported by the Center for Infectious Disease  
461 Control of the Netherlands National Institute for Public Health and the Environment.

462

#### 463 **CONFLICT OF INTERESTS**

464 No conflict of interests.

465

#### 466 **DATA AVAILABILITY**

467 Antibody sequences will be available on request to the corresponding author. Variable domain  
468 sequences of heavy and light chains were uploaded in Genbank under accession numbers  
469 MZ170096, MZ170095, MZ170094, and MZ170097 for NAb 05A1, 05A2, 05A3, and 07A1  
470 respectively.

471

472 **METHODS**473 *Isolation of rabbit Peripheral blood mononuclear cells*

474 Blood of immunized rabbits was used for Peripheral blood mononuclear cells (PBMC)  
475 isolation through ficoll separation. In short, blood was diluted 1:1 with PBS, loaded on a ficoll  
476 layer, and centrifuged for 30 min at room temperature (RT) at 400xg with an acceleration  
477 speed of 7 and a deceleration speed of 0. PBMCs were isolated, washed with PBS and  
478 subsequently re-suspended in 1-2 mL of ACK buffer (Thermo Fisher Scientific) to remove red  
479 blood cells. PBMCs were counted, suspended in fetal calf serum with 10% DMSO and directly  
480 frozen at -150°C.

481

482 *Env protein design, production, and purification*

483 All SOSIP trimers contained the previously described SOSIP mutations(8) and were  
484 further stabilized with additional mutations yielding SOSIP.v4.2 (E66K + A316W) trimers(10).  
485 ConM and SHIVp3 SOSIP trimers contained additional mutations (SOSIP.v9) described  
486 elsewhere(48–50). All SOSIP constructs were cloned into a pPPI4 expression vector(51).  
487 Mutant variants were generated by the use of the Q5 site-directed mutagenesis kit (New  
488 England Biolabs) with specifically designed primer sets and adapted annealing temperatures  
489 for the mutations N88Q, K232T, K236T, K232T+K236T, N611Q, N616Q, N637Q, D602N, N624D  
490 and E662A. D7324 tags were incorporated directly C-terminally of residue 664 in each of the  
491 plasmids(8). Additionally we replaced the D7324 tag C-terminally of residue 664 with an Avi-  
492 tag in the AMC008 SOSIP.v.4.2 construct for biotinylation (16). For BLI and SPR experiments a  
493 His-tag was incorporated into AMC008 SOSIP.v4.2, and the AMC008 SOSIP.v4.2 D620N,  
494 N624D, and E662A mutant plasmids, replacing the D7324 tag(2).

495 All SOSIP trimer variants were produced as described before(6, 8, 10, 52, 53). In short,  
496 SOSIP trimers were transiently expressed together with furin from a separate expression  
497 plasmid (ratio 4:1) in HEK293F cells (Invitrogen, catalog number R79009). The SOSIP trimers  
498 were harvested by spinning for 20 min at 4000xg. The supernatant was 0.22  $\mu$ M steritop-  
499 vacuum-filtered before purification by gravity-driven chromatography on a PGT145 antibody-  
500 conjugated Sepharose column. Env proteins were eluted with 3M  $Mg_2Cl_2$  pH 7.8, directly into  
501 neutralization buffer (20 mM TrisHCl pH8.0, 75mM NaCl). After purification, Env proteins were  
502 concentrated with Vivaspin 100kD filters (GE healthcare), to a final volumes of <500  $\mu$ L.  
503 AMC008 SOSIP.v4.2-Avi was biotinylated to allow conjugation for FACS analysis. BirA biotin  
504 protein ligase (Avidity) was used for the biotinylation.

505

#### 506 *Antibody production and purification*

507 HEK293F cells (Invitrogen, catalog number R79009) were transfected to produce mAbs  
508 as described previously(16). In short, 62.5  $\mu$ g of each heavy and light chain Ab DNA were co-  
509 transfected transiently in 250 mL HEK293F cells. Cell supernatant was harvested at 5 days by  
510 spinning down for 20 min at 4000xg and subsequent vacuum filtration with a 0.22  $\mu$ M steritop  
511 filter. Abs were purified from the culture supernatant by gravity-driven chromatography on a  
512 Protein G (Thermo Fisher Scientific) affinity column. After addition of the supernatant,  
513 columns were washed twice with PBS before elution with 9 mL 0.1 M glycine, pH 2.0. Eluted  
514 Abs were collected in 1 mL 1 M Tris-HCl pH 7.8. After elution Abs were concentrated, by the  
515 use of 100kD vivaspin (GE healthcare) filters, to a final volume of <200  $\mu$ L.

516 We named the isolated mAbs as described by McCoy *et al*, 2016(16): in this system  
517 each mAb is numbered according to their rabbit ID followed by a unique alphabetical lineage

518 identifier (A, B, C, etc.). Distinct lineage members received an additional number (A1, A2, A3,  
519 etc.).

520

#### 521 *Single B cell sorting*

522 Single B cells were selected and sorted as previously described(16). Briefly, biotinylated  
523 AMC008 SOSIP.v4.2-Avi Env proteins were conjugated to Strep-APC and Strep-FITC (both  
524 Thermo Fisher Scientific). Mouse-anti-rabbit IgG Ab conjugated to PE stained IgG on memory  
525 B cells (Southern Biotech). Conjugated Env protein was mixed with PBMCs to allow binding.  
526 We first selected IgG<sup>+</sup> cells and within this population sorted single B cells, positive for both  
527 APC and FITC conjugated AMC008.v4.2 Env trimer into a lysis buffer (RNAse inhibitor (20U)  
528 (Thermo Fisher Scientific), 5X First strand superscript III buffer (Invitrogen), 0.1 M DTT  
529 (Invitrogen), and MQ). Sorted cells were immediately frozen at -80°C.

530

#### 531 *Single cell Ab RT-PCR, variable region gene amplification and cloning*

532 6 µL RT-PCR reaction mixture (random hex primers (200 ng) (Thermo Fisher Scientific),  
533 dNTP mix (2 mM each) (New England Biolabs), 50U Superscript III RTase, and MQ) was added  
534 directly to the sorted single B cells. The following PCR program was used to convert RNA into  
535 cDNA: 42°C 10 min; 25°C 10 min; 50°C 60 min; 95°C 5 min. RT-PCR plates were used directly  
536 for variable region gene amplification using two subsequent PCR reactions. For both PCR  
537 reactions 13 µL of PCR mix (MQ, 10x PCR reaction buffer, dNTPs (10 mM), 0.25U Hotstar Plus  
538 polymerase (Qiagen), forward primer (25 mM), reverse primer (25 mM)) was added  
539 subsequently to the RT-PCR plate and the PCR1 plate. For PCR1, 2 µL of RT-PCR product was  
540 added to this mix. PCR 1 was run at 95°C for 5 min (50 cycles of: 94°C 30 seconds; 58°C 30 sec;

541 72°C 1 min) 72°C 10 min. For the heavy chain amplification, the annealing temperature was  
542 adapted to 48°C. For PCR2, 2 µL of PCR1 product was added to the PCR mix and DNA was  
543 amplified at 95°C for 5 min; (50 cycles: 94°C 30 sec; 55°C 30 sec; 72°C 1 min) 72°C 10 min. A  
544 final PCR3 reaction using 1 µL of PCR2 product was performed in MQ, 5x Phusion PCR buffer,  
545 dNTPs (10 mM), forward primers (25 mM), reverse primers (25 mM), 0.2U Phusion high fidelity  
546 polymerase (New England Biolabs). The following PCR program was run; 98°C 30 sec; (35  
547 cycles: 98°C 5 sec; 68°C 15 sec; 72°C 20 sec); 72°C 5 min.

548 Heavy and light chain amplified variable regions were cloned into vectors expressing  
549 respectively the heavy or light chain constant region of rabbit Abs by Gibson cloning. In short,  
550 1 µL vector (45 ng) was incubated with 1 µL PCR3 product and 2x Gibson mix (T5 exonuclease  
551 (0.2U) (Epibio), Phusion polymerase (12.5U) (New England Biolabs), Taq DNA ligase (2000U)  
552 (New England Biolabs), gibson reaction buffer (0.5 grams PEG-8000 (Sigma Life Sciences), 1 M  
553 Tris/ HCl pH 7.5, 1 M MgCl<sub>2</sub>, 1 M DTT, 100 mM dNTPs, 50 mM NAD (New England Biolabs),  
554 MQ)) for 60 min at 50°C.

555

#### 556 *Mutant virus construction and production*

557 The infectious molecular clone (IMC) encoding for replication-competent virus with  
558 AMC008 Env has been described before(10). First, the AMC008 *env* fragment was transferred  
559 to pUC18 by traditional cloning methods using restriction enzymes Sall and BamHI (New  
560 England Biolabs). Mutations were then generated using the Q5 mutagenesis kit (New England  
561 Biolabs). Mutated AMC008 *env* fragments were cloned back into the original IMC by Gibson  
562 reactions. To produce virus stocks, HEK293T cells (ATCC, CRL-11268) were transfected with

563 the IMCs using lipofectamin2000 (Invitrogen) and supernatants containing viruses were  
564 harvested 3 days later. Supernatants were directly frozen at -80°C.

565

#### 566 *Neutralization assays*

567 Neutralization assays were executed as described previously(8, 15). In short, 1 in 3  
568 dilution series were made of the various mAbs starting at end-concentrations varying from 50  
569 µg/mL to 100 µg/mL. Virus of interest was added to the diluted mAb, and incubated for 1 h at  
570 RT. After incubation the mixture was added to TZM-bl reporter cells (obtained through the  
571 NIH AIDS Reagent Program, Division of AIDS, NIAID, NIH from Dr. John C. Kappes, and Dr.  
572 Xiaoyun Wu) and incubated for 3 days at 37°C. IC<sub>50</sub> values were determined as the  
573 concentration at which infectivity was inhibited by 50%.

574 For the decay neutralization assays, virus and mAb mixtures were incubated for 1 h, 3  
575 h, 6 h, and 24 h at 37°C before addition to the TZM-bl reporter cells.

576

#### 577 *Negative stain electron microscopy*

578 Complex formation was performed by incubating AMC008 SOSIP.v4.2 trimers with a 6-  
579 fold molar excess of fab for 3 h at RT. Complexes were subsequently diluted to 0.03 mg/mL in  
580 1X TBS pH 7.4 to achieve optimal particle density. Copper mesh grids were plasma cleaned for  
581 20s using a mix of Argon and Oxygen gas and samples were stained with 2% uranyl formate  
582 for 50s. For each dataset, a FEI Tecnai Spirit (120 kEV) with a Tietz (4k x 4k) camera was used  
583 in conjunction with the automated data collection software package, Legion(54). Data  
584 collection parameters include: a magnification of 56,000x, a defocus of -1.5 µm, a pixel size of  
585 2.05 Å per pixel, and a dose of 25 e<sup>-</sup>/Å<sup>2</sup>. Resulting images were stored in Appion(55), particles

586 were picked with DoGPicker(56), stacked with a box size of 192 pixels, and processed using  
587 RELION(57). UCSF Chimera(58) was used for map segmentation and map/model docking.

588

#### 589 *Binding and competition ELISAs*

590 Binding ELISA experiments were performed as previously described(2, 4). In short,  
591 ELISA plates were coated overnight with 100 µg Ghalanthus Nivalis Lectin (GNL) in 0.1 M  
592 NaHCO<sub>3</sub> pH 8.6 and blocked using casein (Thermo Fisher Scientific) at RT for 1 h after washing  
593 off the GNL with Tris Buffered Saline (TBS). Env trimers were added at 2 µg/mL and incubated  
594 at RT for 2 h. Subsequently, Ab 3-fold serial dilutions were added for 2 h at RT at starting  
595 concentrations ranging from 1 µg/mL up to 10 µg/mL. After washing with TBS a 1:3000 dilution  
596 of goat-anti-human or goat-anti-rabbit Horseradish Peroxidase (HRP) (SeraCare, 1 µg/mL)  
597 conjugated Ab was added and incubated at RT for 1 h. After washing with TBS+0.05% Tween-  
598 20, ELISA plates were developed using 1% 3,3',5,5'-tetranethylbenzidine (Sigma-Aldrich),  
599 0.01% H<sub>2</sub>O<sub>2</sub>, 100 mM sodium acetate, and 100 mM citric acid and reactions were stopped  
600 after 3 min using 0.8 M H<sub>2</sub>SO<sub>4</sub>.

601 For HEK293T supernatant ELISAs the same protocol was followed however, 50 µL of  
602 HEK293T supernatant containing unpurified mAb was added instead of purified Abs.

603 For competition ELISA, His-tagged Env trimers were added at 2 µg/mL to pre-coated  
604 Ni-NTA plates (Qiagen) and left at RT for 2 h. Blocking was achieved in 2% milk in TBS at RT for  
605 1 h. The primary Ab (competitor) was added at excess (10 µg/mL) in 50 µl and incubated for  
606 30 min at RT before the analyte Ab was added at a previously determined EC<sub>70</sub> concentration  
607 in 50 µL and left at RT for another 1.5 h. Statistical significance was determined using an one-

608 way ANOVA multiple comparisons test (Prism) comparing the sample without competitor to  
609 the corresponding sample with competitor present.

610

611 *Octet K2 Bio-Layer Interferometry (BLI) kinetics and binding experiments*

612 All assays were conducted on the Octet K2 system (Bioforte). 6 µg/ml of his-tagged  
613 AMC008 SOSIP.v4.2-His Env trimer was captured on NiNTA sensors (Bioforte) for 600s after  
614 baseline determination in PBS with 0.01% Bovine Serum Albumine and 0.002% Tween for 60s.  
615 Association of a serial dilution of rabbit mAbs starting at 15 µg/mL was measured for 600s by  
616 dipping the AMC008 SOSIP.v4.2 trimer loaded sensor into a well containing mAb.  
617 Subsequently dissociation was measured in PBS 0.01% BSA 0.002% Tween buffer for 600s.  
618 Binding kinetics (Kd, ka and kd) were determined using a 1:1 fit model with independent fitting  
619 of Rmax (Octet Data Analysis software, Bioforte). Regeneration of the sensors was achieved  
620 through alternating cycles of 5s in low pH glycine buffer and a neutralization buffer (PBS,  
621 0.01% BSA, 0.002% Tween). After regeneration sensors were used to re-capture Env protein.

622 For competition analysis, after association of the competitor mAb to the SOSIP trimer  
623 bound to NiNTA sensors, a second 600s association step was incorporated for the analyte  
624 mAb. % residual binding was calculated as follows; shift in nm at 600s of analyte  
625 binding\*100)/nm shift of analyte in the absence of competitor binding.

626

627 *Surface plasmon resonance (SPR)*

628 Surface Plasmon Resonance (SPR) experiments were done for kinetic and competition  
629 analysis of rabbit mAbs, as previously described (34). All assays were conducted on Biacore  
630 3000 at 25°C. In all assays HBS-EP (10mM HEPES [pH7.4], 150 mM NaCl, 3 mM EDTA, 0.002%

631 P20 surfactant) was used as running buffer (GE Healthcare). Briefly, Anti-his Ab was covalently  
632 immobilized (15,000 RU) in all flow cells of a CM5 sensor chip, by standard amine-coupling.  
633 AMC008 SOSIP.v4.2-His Env trimer was captured on the anti-His-CM5 surface for both and  
634 competition analysis.

635 Competition assays were carried out with mAbs binding to the CD4bs (VRC01), gp120  
636 V3-glycan (PGT121), and the gp120-gp140 interface (PGT151, 35O22, and ACS202). In the  
637 competition assays, mAbs were sequentially injected in the same cycle: the first Ab was  
638 injected for 200s immediately followed by the second Ab, at a flow rate of 30  $\mu$ l/min.  
639 Dissociation was followed for 300s during the second injection. In addition, the second mAb  
640 was injected alone in a separate cycle.

641 The trimer-immobilization levels and mAb concentrations were optimized earlier to  
642 yield maximum self-competition. Rabbit mAbs (05A1, 05A2, 05A3), PGT121, PGT151, and  
643 ACS202 showed 5-15% residual binding at a concentration of 1  $\mu$ M and trimer density of 500  
644 RU, whereas, VRC01 and 35O22, self-competed (15-20% residual binding) at a concentration  
645 of 1.5  $\mu$ M and a density of  $\sim$ 250 RU of AMC008 SOSIP.v4.2 trimer. Those mAb concentrations  
646 were used thereafter in the cross-competitions; and for rabbit mAbs and VRC01 or 35O22, the  
647 trimer was captured to a level of 250 RU, whereas the other Abs (PGT121, PGT151, and  
648 ACS202) were done at a trimer capture level of 500 RU. The residual binding was calculated  
649 as (Response difference at 200s for the second Ab)/(Response difference at 200s for the same,  
650 second Ab when injected as a single Ab in a separate cycle)\*100 (%). Significance was  
651 determined by an one-way ANOVA multiple comparisons test (prism) comparing the sample  
652 without competitor to the corresponding sample with competitor present.

653

654 *Full length SOSIP binding experiment*

655 Surface expressed full length AMC008.v4.2 SOSIP Env trimers were obtained by co-  
656 transfection of 10 µg gp160 SOSIP expression plasmid(39) and 2.5 µg Furin expression plasmid  
657 into 1.75x10<sup>6</sup> cells/mL HEK293F cells as described above. 60-65 h post transfection cells were  
658 spun down at 4000xg. 1\*10<sup>5</sup> 293F cells were added to each well of serially diluted mAbs and  
659 incubated for 2 h on ice. Cells were washed twice with PBS and subsequently stained in a  
660 volume of 20 µl containing 1:70 alexa-647 (2 mg/mL) conjugated mouse anti-human IgG (for  
661 2G12 and PGT145 controls) (Invitrogen), or 1:70 PE (0.1 mg/mL) conjugated mouse anti-rabbit  
662 IgG (Southern Biotech). Cells were stained for 45 min on ice and covered in foil and  
663 subsequently washed with PBS and re-suspended in 100 µL PBS and analyzed using a FACS  
664 canto II analyzer (BD). Maximum mean fluorescent intensity (MFI) was calculated and plotted  
665 for each of the samples.

666

667 **References:**

- 668 1. Dubrovskaya V, Tran K, Ozorowski G, Guenaga J, Wilson R, Bale S, Cottrell CA, Turner HL, Seabright G,  
669 O'Dell S, Torres JL, Yang L, Feng Y, Leaman DP, Vázquez Bernat N, Liban T, Louder M, McKee K, Bailer  
670 RT, Movsesyan A, Doria-Rose NA, Pancera M, Karlsson Hedestam GB, Zwick MB, Crispin M, Mascola JR,  
671 Ward AB, Wyatt RT. 2019. Vaccination with Glycan-Modified HIV NFL Envelope Trimer-Liposomes Elicits  
672 Broadly Neutralizing Antibodies to Multiple Sites of Vulnerability. *Immunity* 51:915-929.e7.
- 673 2. Brouwer PJM, Antanasijevic A, Berndsen Z, Yasmeeen A, Fiala B, Bijl TPL, Bontjer I, Bale JB, Sheffler W,  
674 Allen JD, Schorcht A, Burger JA, Camacho M, Ellis D, Cottrell CA, Behrens AJ, Catalano M, del Moral-  
675 Sánchez I, Ketas TJ, LaBranche C, van Gils MJ, Sliepen K, Stewart LJ, Crispin M, Montefiori DC, Baker D,  
676 Moore JP, Klasse PJ, Ward AB, King NP, Sanders RW. 2019. Enhancing and shaping the immunogenicity  
677 of native-like HIV-1 envelope trimers with a two-component protein nanoparticle. *Nat Commun* 10.
- 678 3. Rutten L, Lai YT, Blokland S, Truan D, Bisschop IJM, Strokappe NM, Koornneef A, van Manen D, Chuang

- 679 GY, Farney SK, Schuitemaker H, Kwong PD, Langedijk JPM. 2018. A Universal Approach to Optimize the  
680 Folding and Stability of Prefusion-Closed HIV-1 Envelope Trimers. *Cell Rep* 23:584–595.
- 681 4. Derking R, Ozorowski G, Sliepen K, Yasmineen A, Cupo A, Torres JL, Julien JP, Lee JH, van Montfort T, de  
682 Taeye SW, Connors M, Burton DR, Wilson IA, Klasse PJ, Ward AB, Moore JP, Sanders RW. 2015.  
683 Comprehensive Antigenic Map of a Cleaved Soluble HIV-1 Envelope Trimer. *PLoS Pathog* 11:1–22.
- 684 5. Sanders RW, Vesanen M, Schuelke N, Master A, Schiffner L, Kalyanaraman R, Paluch M, Berkhout B,  
685 Maddon PJ, Olson WC, Lu M, Moore JP. 2002. Stabilization of the Soluble, Cleaved, Trimeric Form of the  
686 Envelope Glycoprotein Complex of Human Immunodeficiency Virus Type 1. *J Virol*  
687 <https://doi.org/10.1128/jvi.76.17.8875-8889.2002>.
- 688 6. Sanders RW, Van Gils MJ, Derking R, Sok D, Ketas TJ, Burger JA, Ozorowski G, Cupo A, Simonich C, Goo  
689 L, Arendt H, Kim HJ, Lee JH, Pugach P, Williams M, Debnath G, Moldt B, Van Breemen MJ, Isik G,  
690 Medina-Ramírez M, Back JW, Koff WC, Julien JP, Rakasz EG, Seaman MS, Guttman M, Lee KK, Klasse PJ,  
691 LaBranche C, Schief WR, Wilson IA, Overbaugh J, Burton DR, Ward AB, Montefiori DC, Dean H, Moore  
692 JP. 2015. HIV-1 neutralizing antibodies induced by native-like envelope trimers. *Science* (80- ) 349.
- 693 7. Hladik F, McElrath MJ. 2008. Setting the stage: Host invasion by HIV. *Nat Rev Immunol*.
- 694 8. Sanders RW, Derking R, Cupo A, Julien JP, Yasmineen A, de Val N, Kim HJ, Blattner C, de la Peña AT,  
695 Korzun J, Golabek M, de los Reyes K, Ketas TJ, van Gils MJ, King CR, Wilson IA, Ward AB, Klasse PJ,  
696 Moore JP. 2013. A Next-Generation Cleaved, Soluble HIV-1 Env Trimer, BG505 SOSIP.664 gp140,  
697 Expresses Multiple Epitopes for Broadly Neutralizing but Not Non-Neutralizing Antibodies. *PLoS Pathog*  
698 9.
- 699 9. Torrents de la Peña A, de Taeye SW, Sliepen K, LaBranche CC, Burger JA, Schermer EE, Montefiori DC,  
700 Moore JP, Klasse PJ, Sanders RW. 2018. Immunogenicity in Rabbits of HIV-1 SOSIP Trimers from Clades  
701 A, B, and C, Given Individually, Sequentially, or in Combination. *J Virol* 92.
- 702 10. de Taeye SW, Ozorowski G, Torrents de la Peña A, Guttman M, Julien J-P, van den Kerkhof TLGM,  
703 Burger JA, Pritchard LK, Pugach P, Yasmineen A, Crampton J, Hu J, Bontjer I, Torres JL, Arendt H,  
704 DeStefano J, Koff WC, Schuitemaker H, Eggink D, Berkhout B, Dean H, LaBranche C, Crotty S, Crispin M,  
705 Montefiori DC, Klasse PJ, Lee KK, Moore JP, Wilson IA, Ward AB, Sanders RW. 2015. Immunogenicity of  
706 Stabilized HIV-1 Envelope Trimers with Reduced Exposure of Non-neutralizing Epitopes. *Cell* 163:1702–

- 707 15.
- 708 11. Pauthner M, Havenar-Daughton C, Sok D, Nkolola JP, Bastidas R, Boopathy A V., Carnathan DG,  
709 Chandrashekar A, Cirelli KM, Cottrell CA, Eroshkin AM, Guenaga J, Kaushik K, Kulp DW, Liu J, McCoy LE,  
710 Oom AL, Ozorowski G, Post KW, Sharma SK, Steichen JM, de Taeye SW, Tokatlian T, Torrents de la Peña  
711 A, Butera ST, LaBranche CC, Montefiori DC, Silvestri G, Wilson IA, Irvine DJ, Sanders RW, Schief WR,  
712 Ward AB, Wyatt RT, Barouch DH, Crotty S, Burton DR. 2017. Elicitation of Robust Tier 2 Neutralizing  
713 Antibody Responses in Nonhuman Primates by HIV Envelope Trimer Immunization Using Optimized  
714 Approaches. *Immunity* 46:1073-1088.e6.
- 715 12. Bale S, Martiné A, Wilson R, Behrens AJ, Fourn V Le, Val N de, Sharma SK, Tran K, Torres JL, Girod PA,  
716 Ward AB, Crispin M, Wyatt RT. 2018. Cleavage-independent HIV-1 trimers from CHO cell lines elicit  
717 robust autologous tier 2 neutralizing antibodies. *Front Immunol* 9.
- 718 13. Burton DR. 2017. What are the most powerful immunogen design vaccine strategies?: Reverse  
719 vaccinology 2.0 shows great promise. *Cold Spring Harb Perspect Biol*  
720 <https://doi.org/10.1101/cshperspect.a030262>.
- 721 14. van Haaren MM, van den Kerkhof TLGM, van Gils MJ. 2017. Natural infection as a blueprint for rational  
722 HIV vaccine design. *Hum Vaccines Immunother* 13:229–236.
- 723 15. Klasse PJ, Ketas TJ, Cottrell CA, Ozorowski G, Debnath G, Camara D, Francomano E, Pugach P, Ringe RP,  
724 LaBranche CC, van Gils MJ, Bricault CA, Barouch DH, Crotty S, Silvestri G, Kasturi S, Pulendran B, Wilson  
725 IA, Montefiori DC, Sanders RW, Ward AB, Moore JP. 2018. Epitopes for neutralizing antibodies induced  
726 by HIV-1 envelope glycoprotein BG505 SOSIP trimers in rabbits and macaques. *PLoS Pathog* 14.
- 727 16. McCoy LE, van Gils MJ, Ozorowski G, Messmer T, Briney B, Voss JE, Kulp DW, Macauley MS, Sok D,  
728 Pauthner M, Menis S, Cottrell CA, Torres JL, Hsueh J, Schief WR, Wilson IA, Ward AB, Sanders RW,  
729 Burton DR. 2016. Holes in the Glycan Shield of the Native HIV Envelope Are a Target of Trimer-Elicited  
730 Neutralizing Antibodies. *Cell Rep* 16:2327–2338.
- 731 17. Cottrell CA, van Schooten J, Bowman CA, Yuan M, Oyen D, Shin M, Morpurgo R, van der Woude P, van  
732 Breemen M, Torres JL, Patel R, Gross J, Sewall LM, Copps J, Ozorowski G, Nogal B, Sok D, Rakasz EG,  
733 Labranche C, Vigdorovich V, Christley S, Carnathan DG, Sather DN, Montefiori D, Silvestri G, Burton DR,  
734 Moore JP, Wilson IA, Sanders RW, Ward AB, van Gils MJ. 2020. Mapping the immunogenic landscape of

- 735 near-native HIV-1 envelope trimers in non-human primates. *PLoS Pathog* 16:e1008753.
- 736 18. Ringe RP, Pugach P, Cottrell CA, LaBranche CC, Seabright GE, Ketas TJ, Ozorowski G, Kumar S, Schorcht  
737 A, van Gils MJ, Crispin M, Montefiori DC, Wilson IA, Ward AB, Sanders RW, Klasse PJ, Moore JP. 2018.  
738 Closing and Opening Holes in the Glycan Shield of HIV-1 Envelope Glycoprotein SOSIP Trimers Can  
739 Redirect the Neutralizing Antibody Response to the Newly Unmasked Epitopes. *J Virol* 93.
- 740 19. Nogal B, Bianchi M, Cottrell CA, Kirchdoerfer RN, Sewall LM, Turner HL, Zhao F, Sok D, Burton DR,  
741 Hangartner L, Ward AB. 2019. Mapping polyclonal antibody responses in non-human primates  
742 vaccinated with HIV Env trimer subunit vaccines. *bioRxiv* 833715.
- 743 20. Bianchi M, Turner HL, Nogal B, Cottrell CA, Oyen D, Pauthner M, Bastidas R, Nedellec R, McCoy LE,  
744 Wilson IA, Burton DR, Ward AB, Hangartner L. 2018. Electron-Microscopy-Based Epitope Mapping  
745 Defines Specificities of Polyclonal Antibodies Elicited during HIV-1 BG505 Envelope Trimer  
746 Immunization. *Immunity* <https://doi.org/10.1016/j.immuni.2018.07.009>.
- 747 21. Yasmeen A, Ringe R, Derking R, Cupo A, Julien JP, Burton DR, Ward AB, Wilson IA, Sanders RW, Moore  
748 JP, Klasse PJ. 2014. Differential binding of neutralizing and non-neutralizing antibodies to native-like  
749 soluble HIV-1 Env trimers, uncleaved Env proteins, and monomeric subunits. *Retrovirology* 11:41.
- 750 22. Steckbeck JD, Orlov I, Chow A, Grieser H, Miller K, Bruno J, Robinson JE, Montelaro RC, Cole KS. 2005.  
751 Kinetic Rates of Antibody Binding Correlate with Neutralization Sensitivity of Variant Simian  
752 Immunodeficiency Virus Strains. *J Virol* 79:12311–12320.
- 753 23. Wibmer CK, Gorman J, Anthony CS, Mkhize NN, Druz A, York T, Schmidt SD, Labuschagne P, Louder MK,  
754 Bailer RT, Abdool Karim SS, Mascola JR, Williamson C, Moore PL, Kwong PD, Morris L. 2016. Structure of  
755 an N276-Dependent HIV-1 Neutralizing Antibody Targeting a Rare V5 Glycan Hole Adjacent to the CD4  
756 Binding Site. *J Virol* 90:10220–10235.
- 757 24. Pan R, Sampson JM, Chen Y, Vaine M, Wang S, Lu S, Kong X-P. 2013. Rabbit Anti-HIV-1 Monoclonal  
758 Antibodies Raised by Immunization Can Mimic the Antigen-Binding Modes of Antibodies Derived from  
759 HIV-1-Infected Humans. *J Virol* 87:10221–10231.
- 760 25. Voss JE, Andrabi R, McCoy LE, de Val N, Fuller RP, Messmer T, Su CY, Sok D, Khan SN, Garces F, Pritchard  
761 LK, Wyatt RT, Ward AB, Crispin M, Wilson IA, Burton DR. 2017. Elicitation of Neutralizing Antibodies  
762 Targeting the V2 Apex of the HIV Envelope Trimer in a Wild-Type Animal Model. *Cell Rep* 21:222–235.

- 763 26. Duan H, Chen X, Boyington JC, Cheng C, Zhang Y, Jafari AJ, Stephens T, Tsybovsky Y, Kalyuzhnyi O, Zhao  
764 P, Menis S, Nason MC, Normandin E, Mukhamedova M, DeKosky BJ, Wells L, Schief WR, Tian M, Alt FW,  
765 Kwong PD, Mascola JR. 2018. Glycan Masking Focuses Immune Responses to the HIV-1 CD4-Binding Site  
766 and Enhances Elicitation of VRC01-Class Precursor Antibodies. *Immunity* 49:301-311.e5.
- 767 27. Hessel AJ, Powell R, Jiang X, Luo C, Weiss S, Dussupt V, Itri V, Fox A, Shapiro MB, Pandey S, Cheever T,  
768 Fuller DH, Park B, Krebs SJ, Totrov M, Haigwood NL, Kong XP, Zolla-Pazner S. 2019. Multimeric Epitope-  
769 Scaffold HIV Vaccines Target V1V2 and Differentially Tune Polyfunctional Antibody Responses. *Cell Rep*  
770 28:877-895.e6.
- 771 28. Rantalainen K, Berndsen ZT, Antanasijevic A, Schiffner T, Zhang X, Lee WH, Torres JL, Zhang L, Irimia A,  
772 Copps J, Zhou KH, Kwon YD, Law WH, Schramm CA, Verardi R, Krebs SJ, Kwong PD, Doria-Rose NA,  
773 Wilson IA, Zwick MB, Yates JR, Schief WR, Ward AB. 2020. HIV-1 Envelope and MPER Antibody  
774 Structures in Lipid Assemblies. *Cell Rep* 31:107583.
- 775 29. Lee JH, Leaman DP, Kim AS, Torrents De La Penã A, Sliepen K, Yasmeen A, Derking R, Ramos A, De Taeye  
776 SW, Ozorowski G, Klein F, Burton DR, Nussenzweig MC, Pognard P, Moore JP, Klasse PJ, Sanders RW,  
777 Zwick MB, Wilson IA, Ward AB. 2015. Antibodies to a conformational epitope on gp41 neutralize HIV-1  
778 by destabilizing the Env spike. *Nat Commun* 6.
- 779 30. Kong L, Lee JH, Doores KJ, Murin CD, Julien JP, McBride R, Liu Y, Marozsan A, Cupo A, Klasse PJ,  
780 Hoffenberg S, Caulfield M, King CR, Hua Y, Le KM, Khayat R, Deller MC, Clayton T, Tien H, Feizi T,  
781 Sanders RW, Paulson JC, Moore JP, Stanfield RL, Burton DR, Ward AB, Wilson IA. 2013. Supersite of  
782 immune vulnerability on the glycosylated face of HIV-1 envelope glycoprotein gp120. *Nat Struct Mol*  
783 *Biol* 20:796–803.
- 784 31. Pejchal R, Doores KJ, Walker LM, Khayat R, Huang PS, Wang SK, Stanfield RL, Julien JP, Ramos A, Crispin  
785 M, Depetris R, Katpally U, Marozsan A, Cupo A, Malveste S, Liu Y, McBride R, Ito Y, Sanders RW,  
786 Ogohara C, Paulson JC, Feizi T, Scanlan CN, Wong CH, Moore JP, Olson WC, Ward AB, Pognard P, Schief  
787 WR, Burton DR, Wilson IA. 2011. A potent and broad neutralizing antibody recognizes and penetrates  
788 the HIV glycan shield. *Science* (80- ) 334:1097–1103.
- 789 32. Lavinder JJ, Hoi KH, Reddy ST, Wine Y, Georgiou G. 2014. Systematic characterization and comparative  
790 analysis of the rabbit immunoglobulin repertoire. *PLoS One* 9:1–11.

- 791 33. Kodangattil S, Huard C, Ross C, Li J, Gao H, Mascioni A, Hodawadekar S, Naik S, Min-debartolo J, Visintin  
792 A, Almagro JC. 2014. The functional repertoire of rabbit antibodies and antibody discovery via next-  
793 generation sequencing. *MAbs* 6:628–636.
- 794 34. Van Gils MJ, Van Den Kerkhof TLGM, Ozorowski G, Cottrell CA, Sok D, Pauthner M, Pallesen J, De Val N,  
795 Yasmeen A, De Teye SW, Schorcht A, Gumbs S, Johanna I, Saye-Francisco K, Liang CH, Landais E, Nie X,  
796 Pritchard LK, Crispin M, Kelsoe G, Wilson IA, Schuitemaker H, Klasse PJ, Moore JP, Burton DR, Ward AB,  
797 Sanders RW. 2016. An HIV-1 antibody from an elite neutralizer implicates the fusion peptide as a site of  
798 vulnerability. *Nat Microbiol* 2:423–426.
- 799 35. deCamp A, Hraber P, Bailer RT, Seaman MS, Ochsenbauer C, Kappes J, Gottardo R, Edlefsen P, Self S,  
800 Tang H, Greene K, Gao H, Daniell X, Sarzotti-Kelsoe M, Gorny MK, Zolla-Pazner S, LaBranche CC,  
801 Mascola JR, Korber BT, Montefiori DC. 2014. Global panel of HIV-1 Env reference strains for  
802 standardized assessments of vaccine-elicited neutralizing antibodies. *J Virol* 88:2489–507.
- 803 36. Sliepen K, Han BW, Bontjer I, Mooij P, Garces F, Behrens AJ, Rantalainen K, Kumar S, Sarkar A, Brouwer  
804 PJM, Hua Y, Tolazzi M, Schermer E, Torres JL, Ozorowski G, van der Woude P, de la Peña AT, van  
805 Breemen MJ, Camacho-Sánchez JM, Burger JA, Medina-Ramírez M, González N, Alcami J, LaBranche C,  
806 Scarlatti G, van Gils MJ, Crispin M, Montefiori DC, Ward AB, Koopman G, Moore JP, Shattock RJ, Bogers  
807 WM, Wilson IA, Sanders RW. 2019. Structure and immunogenicity of a stabilized HIV-1 envelope trimer  
808 based on a group-M consensus sequence. *Nat Commun* <https://doi.org/10.1038/s41467-019-10262-5>.
- 809 37. Falkowska E, Le KM, Ramos A, Doores KJ, Lee JH, Blattner C, Ramirez A, Derking R, vanGils MJ, Liang CH,  
810 McBride R, von Bredow B, Shivatare SS, Wu CY, Chan-Hui PY, Liu Y, Feizi T, Zwick MB, Koff WC, Seaman  
811 MS, Swiderek K, Moore JP, Evans D, Paulson JC, Wong CH, Ward AB, Wilson IA, Sanders RW, Poignard P,  
812 Burton DR. 2014. Broadly neutralizing HIV antibodies define a glycan-dependent epitope on the  
813 prefusion conformation of gp41 on cleaved envelope trimers. *Immunity* 40:657–668.
- 814 38. Blattner C, Lee JH, Sliepen K, Derking R, Falkowska E, delaPeña AT, Cupo A, Julien JP, vanGils M, Lee PS,  
815 Peng W, Paulson JC, Poignard P, Burton DR, Moore JP, Sanders RW, Wilson IA, Ward AB. 2014.  
816 Structural delineation of a quaternary, cleavage-dependent epitope at the gp41-gp120 interface on  
817 intact HIV-1 env trimers. *Immunity* 40:669–680.
- 818 39. Torrents de la Peña A, Rantalainen K, Cottrell CA, Allen JD, van Gils MJ, Torres JL, Crispin M, Sanders

- 819 RW, Ward AB. 2019. Similarities and differences between native HIV-1 envelope glycoprotein trimers  
820 and stabilized soluble trimer mimetics. *PLoS Pathog* 15.
- 821 40. Mage RG, Lanning D, Knight KL. 2006. B cell and antibody repertoire development in rabbits: The  
822 requirement of gut-associated lymphoid tissues. *Dev Comp Immunol* 30:137–153.
- 823 41. Klasse PJ, Ketas TJ, Cottrell CA, Ozorowski G, Debnath G, Camara D, Francomano E, Pugach P, Ringe RP,  
824 LaBranche CC, van Gils MJ, Bricault CA, Barouch DH, Crotty S, Silvestri G, Kasturi S, Pulendran B, Wilson  
825 IA, Montefiori DC, Sanders RW, Ward AB, Moore JP. 2018. Epitopes for neutralizing antibodies induced  
826 by HIV-1 envelope glycoprotein BG505 SOSIP trimers in rabbits and macaques. *PLoS Pathog* 14.
- 827 42. Medina-Ramírez M, Garces F, Escolano A, Skog P, de Taeye SW, Del Moral-Sanchez I, McGuire AT,  
828 Yasmeen A, Behrens AJ, Ozorowski G, van den Kerkhof TLGM, Freund NT, Dosenovic P, Hua Y, Gitlin AD,  
829 Cupo A, van der Woude P, Golabek M, Slieden K, Blane T, Kootstra N, van Breemen MJ, Pritchard LK,  
830 Stanfield RL, Crispin M, Ward AB, Stamatatos L, Klasse PJ, Moore JP, Nemazee D, Nussenzweig MC,  
831 Wilson IA, Sanders RW. 2017. Design and crystal structure of a native-like HIV-1 envelope trimer that  
832 engages multiple broadly neutralizing antibody precursors in vivo. *J Exp Med* 214.
- 833 43. Hessel AJ, Malherbe DC, Pissani F, McBurney S, Krebs SJ, Gomes M, Pandey S, Sutton WF, Burwitz BJ,  
834 Gray M, Robins H, Park BS, Sacha JB, LaBranche CC, Fuller DH, Montefiori DC, Stamatatos L, Sather DN,  
835 Haigwood NL. 2016. Achieving Potent Autologous Neutralizing Antibody Responses against Tier 2 HIV-1  
836 Viruses by Strategic Selection of Envelope Immunogens. *J Immunol* 196:3064–3078.
- 837 44. Ozorowski G, Pallesen J, De Val N, Lyumkis D, Cottrell CA, Torres JL, Coppins J, Stanfield RL, Cupo A,  
838 Pugach P, Moore JP, Wilson IA, Ward AB. 2017. Open and closed structures reveal allostery and  
839 pliability in the HIV-1 envelope spike. *Nature* 547:360–361.
- 840 45. Lee JH, Ozorowski G, Ward AB. 2016. Cryo-EM structure of a native, fully glycosylated, cleaved HIV-1  
841 envelope trimer. *Science* (80- ) 351:1043–1048.
- 842 46. Ke Z, Oton J, Qu K, Cortese M, Zila V, McKeane L, Nakane T, Zivanov J, Neufeldt CJ, Cerikan B, Lu JM,  
843 Peukes J, Xiong X, Kräusslich HG, Scheres SHW, Bartenschlager R, Briggs JAG. 2020. Structures and  
844 distributions of SARS-CoV-2 spike proteins on intact virions. *Nature* [https://doi.org/10.1038/s41586-](https://doi.org/10.1038/s41586-020-2665-2)  
845 020-2665-2.
- 846 47. Klasse PJ. 2014. Neutralization of Virus Infectivity by Antibodies: Old Problems in New Perspectives. *Adv*

- 847 Biol 2014:1–24.
- 848 48. Torrents de la Peña A, Julien JP, de Taeye SW, Garces F, Guttman M, Ozorowski G, Pritchard LK, Behrens  
849 AJ, Go EP, Burger JA, Schermer EE, Slieden K, Ketas TJ, Pugach P, Yasmeen A, Cottrell CA, Torres JL,  
850 Vavourakis CD, van Gils MJ, LaBranche C, Montefiori DC, Desaire H, Crispin M, Klasse PJ, Lee KK, Moore  
851 JP, Ward AB, Wilson IA, Sanders RW. 2017. Improving the Immunogenicity of Native-like HIV-1  
852 Envelope Trimers by Hyperstabilization. *Cell Rep* <https://doi.org/10.1016/j.celrep.2017.07.077>.
- 853 49. Guenaga J, Dubrovskaya V, de Val N, Sharma SK, Carrette B, Ward AB, Wyatt RT. 2016. Structure-  
854 Guided Redesign Increases the Propensity of HIV Env To Generate Highly Stable Soluble Trimers. *J Virol*  
855 <https://doi.org/10.1128/jvi.02652-15>.
- 856 50. Kulp DW, Steichen JM, Pauthner M, Hu X, Schiffner T, Liguori A, Cottrell CA, Havenar-Daughton C,  
857 Ozorowski G, Georgeson E, Kalyuzhnyi O, Willis JR, Kubitz M, Adachi Y, Reiss SM, Shin M, De Val N,  
858 Ward AB, Crotty S, Burton DR, Schief WR. 2017. Structure-based design of native-like HIV-1 envelope  
859 trimers to silence non-neutralizing epitopes and eliminate CD4 binding. *Nat Commun*  
860 <https://doi.org/10.1038/s41467-017-01549-6>.
- 861 51. Binley JM, Sanders RW, Clas B, Schuelke N, Master A, Guo Y, Kajumo F, Anselma DJ, Maddon PJ, Olson  
862 WC, Moore JP. 2000. A Recombinant Human Immunodeficiency Virus Type 1 Envelope Glycoprotein  
863 Complex Stabilized by an Intermolecular Disulfide Bond between the gp120 and gp41 Subunits Is an  
864 Antigenic Mimic of the Trimeric Virion-Associated Structure. *J Virol* 74.
- 865 52. Julien JP, Lee JH, Ozorowski G, Hua Y, De La Peña AT, De Taeye SW, Nieuwma T, Cupo A, Yasmeen A,  
866 Golabek M, Pugach P, Klasse PJ, Moore JP, Sanders RW, Ward AB, Wilson IA. 2015. Design and structure  
867 of two HIV-1 clade c SOSIP.664 trimers that increase the arsenal of native-like env immunogens. *Proc*  
868 *Natl Acad Sci U S A* 112.
- 869 53. Pugach P, Ozorowski G, Cupo A, Ringe R, Yasmeen A, de Val N, Derking R, Kim HJ, Korzun J, Golabek M,  
870 de los Reyes K, Ketas TJ, Julien J-P, Burton DR, Wilson IA, Sanders RW, Klasse PJ, Ward AB, Moore JP.  
871 2015. A Native-Like SOSIP.664 Trimer Based on an HIV-1 Subtype B env Gene . *J Virol* 89.
- 872 54. Suloway C, Pulokas J, Fellmann D, Cheng A, Guerra F, Quispe J, Stagg S, Potter CS, Carragher B. 2005.  
873 Automated molecular microscopy: The new Legion system. *J Struct Biol* 151.
- 874 55. Lander GC, Stagg SM, Voss NR, Cheng A, Fellmann D, Pulokas J, Yoshioka C, Irving C, Mulder A, Lau PW,

- 875 Lyumkis D, Potter CS, Carragher B. 2009. Appion: An integrated, database-driven pipeline to facilitate  
876 EM image processing. *J Struct Biol* 166.
- 877 56. Voss NR, Yoshioka CK, Radermacher M, Potter CS, Carragher B. 2009. DoG Picker and TiltPicker:  
878 Software tools to facilitate particle selection in single particle electron microscopy. *J Struct Biol* 166.
- 879 57. Scheres SHW. 2012. RELION: Implementation of a Bayesian approach to cryo-EM structure  
880 determination. *J Struct Biol* 180.
- 881 58. Pettersen EF, Goddard TD, Huang CC, Couch GS, Greenblatt DM, Meng EC, Ferrin TE. 2004. UCSF  
882 Chimera - A visualization system for exploratory research and analysis. *J Comput Chem* 25.
- 883 59. Wagh K, Kreider EF, Li Y, Barbian HJ, Learn GH, Giorgi E, Hraber PT, Decker TG, Smith AG, Gondim M V.,  
884 Gillis L, Wandzilak J, Chuang GY, Rawi R, Cai F, Pellegrino P, Williams I, Overbaugh J, Gao F, Kwong PD,  
885 Haynes BF, Shaw GM, Borrow P, Seaman MS, Hahn BH, Korber B. 2018. Completeness of HIV-1  
886 Envelope Glycan Shield at Transmission Determines Neutralization Breadth. *Cell Rep*  
887 <https://doi.org/10.1016/j.celrep.2018.09.087>.

888

889 **Figure legends:**

890 **Fig 1: Characteristics of mAbs isolated from AMC008 SOSIP trimer immunized rabbits. (A)**

891 Immunization and sample collection scheme (left) and autologous and heterologous serum  
892 neutralization titers at week 22 (right) for four AMC008 SOSIP trimer immunized rabbits.

893 Serum neutralization ID<sub>50</sub> is shown for each animal. (B) Absolute number of mAbs isolated per

894 animal. (C) Individual CDR3 lengths and CDR amino acid junction sequence of heavy and light

895 chains of all isolated mAbs. (D) Individual CDR3 amino acid lengths of the isolated mAbs. (E)

896 Autologous neutralization ability of the isolated mAbs. Neutralization IC<sub>50</sub> values are shown

897 for each of the four NAbs in the accompanying table.

898

899 **Fig 2: Competitive assays of Nabs with bNAbs and non-NAbs to specify an epitope. (A)**

900 Percentage residual binding of NAbs to AMC008 SOSIP trimers in the presence of a competing

38

901 NAb. The % residual binding was calculated as follows: (shift in nm at 600s of 2nd mAb  
902 binding\*100)/nm shift of 2nd mAb in the absence of 1st mAb binding. (B) Competition ELISA  
903 and SPR data of all NAbS with human bNAbS. The percentage of residual binding was  
904 calculated as follows, for ELISA: (average OD450 of a triplo in presence of the 2nd  
905 mAb\*100)/average OD450 of a triplo in absence of the 1st mAb binding, for SPR: (response  
906 difference at 200s for the second Ab)/(Response difference at 200s for the same, second Ab  
907 when injected as a single Ab in a separate cycle) \* 100 (%). Significant results are highlighted  
908 by stars (\*\*=p<0.005 \*\*\*=p<0.0001). SPR was only performed for the 05A family of NAbS. (C)  
909 SPR binding curves of AMC008 SOSIP trimer binding competition between NAbS and the bNAb  
910 ACS2020 that shows the influence of assay directionality. Ab binding is recorded in real-time;  
911 the x-axis indicates the time in seconds. The y-axis shows the response (response units, RU),  
912 proportional to the mass bound. The dissociation starts at 0s. The top three graphs show  
913 binding of ACS202 in presence of competitors 05A1-05A3 (dark red, red, and purple lines),  
914 compared to ACS202 binding in absence of these NAbS (blue lines). The lower three graphs  
915 show a reverse assay set-up, showing NAb 05A1-05A3 binding ability in presence of  
916 competitor ACS202 (blue lines) and in the absence of ACS202 (dark red, red, and purple lines).  
917 (D) Competition results of the four rabbit NAbS with the isolated non-NAbS measured by BLI.  
918 % residual binding was calculated as stated for figure 3A.

919

920 **Fig 3: Epitope mapping of NAbS to the gp41 subunit of Env.** (A) NS-EM 3D reconstructions of  
921 the NAbS fabs in complex with the AMC008 SOSIP trimer. The AMC008 SOSIP trimer structure  
922 is modeled as the ribboned density. The NAbS are shown as white densities. Side and bottom  
923 views are depicted. (B) Alignment of viral sequences tested for neutralization and binding by

924 05A1-05A3 and 07A1. AMC008, AMC009 and SHIV162p3 could be neutralized by the NAb,  
925 whereas the viruses below the line were not neutralized by the NAb. HXB2 amino acid  
926 numbering is indicated on top and lines indicate the NAb binding sites as predicted by NS-EM  
927 imaging. Red boxes show which amino acid residues were mutated in the predicted binding  
928 sites to specify the epitope; D620N, N624D, and E662A. (C) Model of the glycan shield present  
929 on the AMC008 SOSIP trimer with a strain-specific glycan hole indicated in cyan and yellow  
930 due to the absence of PNGS 230 and 234. Image was created with the glycan shield mapping  
931 tool on the Los Alamos database(59). (D) Neutralization ability of NAb to multiple viral  
932 variants. Fold decrease in  $IC_{50}$  values is plotted for each of the NAb and the VRC01 control,  
933 each represented by different colors. The dotted lines indicate a 3-fold threshold compared  
934 to AMC008 WT neutralization  $IC_{50}$  values. (E) Neutralization ability of the NAb for various  
935 AMC008 mutants.  $IC_{50}$  values are indicated in  $\mu\text{g/ml}$ . The bNAb VRC01 is taken along as a  
936 positive control.

937

938 **Fig 4: Epitope mapping of the non-neutralizing antibodies**

939 (A) Binding ability of all isolated mAb to various AMC008 mutants and linear V3 peptide. Fold  
940 change in area under the curve is displayed relative to AMC008.v4.2 binding. Binding to the  
941 V3 peptide is indicated as yes or no.

942 (B) NAb 05A1-05A3 (purple and pink) and 07D2 (grey) were complexed with the AMC008  
943 SOSIP Env and analyzed by NS-EM with the AMC008 SOSIP trimer to show differences in their  
944 binding angle.

945

946 **Fig 5: Analysis of neutralizing and non-neutralization antibody characteristics that might**  
947 **influence neutralization** (A) Binding kinetics of NAbs and non-NAb to the autologous AMC008  
948 SOSIP and heterologous AMC016 SOSIP Env trimers.  $KD$ , on- ( $Ka$ ), and off-rate constants ( $Kd$ )  
949 are shown. NAbs were tested for binding to AMC008 and AMC016 SOSIP Env trimers. Non-  
950 NAbs were only tested for binding to the autologous AMC008 SOSIP trimer. Results were fitted  
951 to a 1:1 kinetics model for analysis. (B) Binding to full length surface expressed AMC008 SOSIP  
952 gp160 Env by mAbs. Maximum median MFI is plotted for each mAb tested. The left panel  
953 shows the binding and expression controls (2G12 and PGT145 respectively). The middle panel  
954 shows binding of the NAbs to full length AMC008 gp160 Env trimers. The right most panel  
955 shows the binding of a selection of non-NAbs to full length AMC008 gp160 Env trimers.

956

957 **Fig 6: NAbs destabilize the trimer as a mechanism of neutralization.** (A) Negative Stain-  
958 Electron Microscopy images of AMC008 SOSIP trimers incubated overnight with the mAb  
959 05A3. The majority of the images displayed the mAb binding with a stoichiometry of 2 mAbs  
960 per trimer (middle image). mAbs binding the monomeric form of the trimer were also  
961 observed (right image). (B) Pre-incubation neutralization experiment to determine the *in vivo*  
962 destabilization ability of the isolated Abs. A neutralization assay was performed in which virus  
963 and Ab mix were incubated for different time periods, up to 24 hours. The fold change in  $IC_{50}$   
964 is shown for each of the Abs. The autologous AMC008 virus and heterologous SHIV162p3  
965 viruses were tested. 3BC315 and PGT126 were tested as positive control and negative control  
966 Abs, respectively. Increased neutralization potency is seen for most of the NAbs and 3BC315  
967 but not 06A1 and PGT126 after the 24 hour incubation step. NN = non-neutralizing.

968

Fig 1

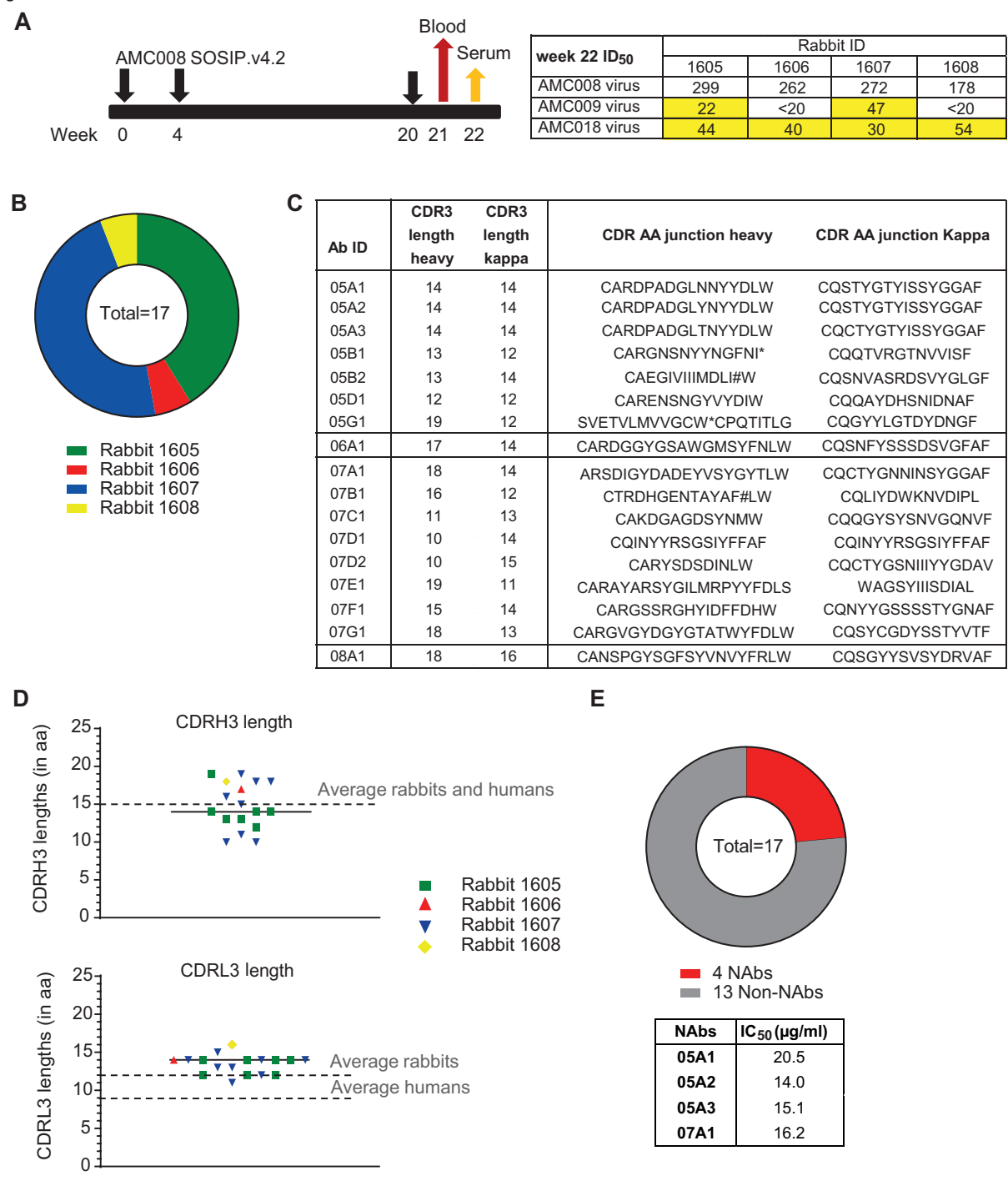


Fig 2

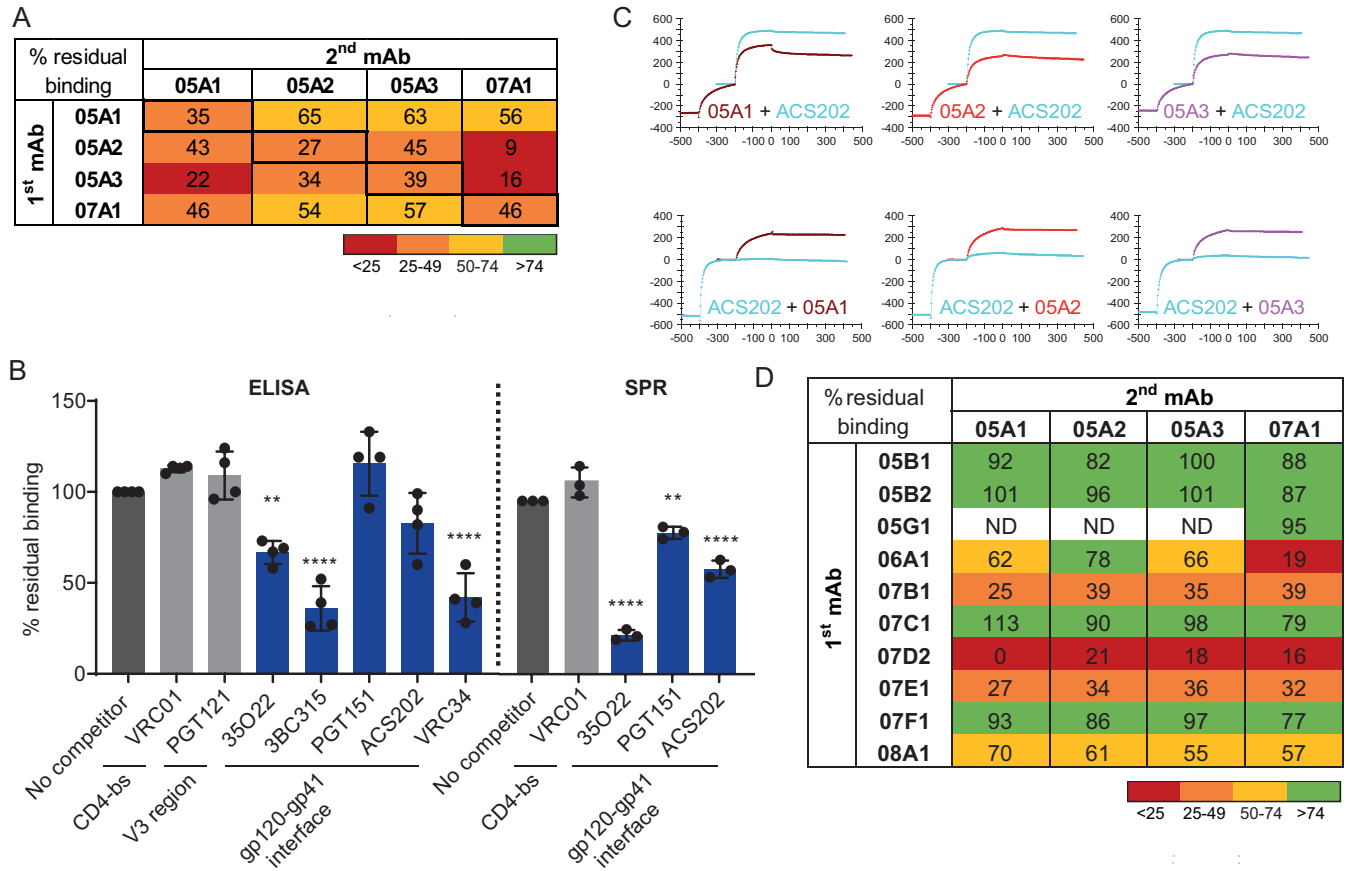


Fig 3

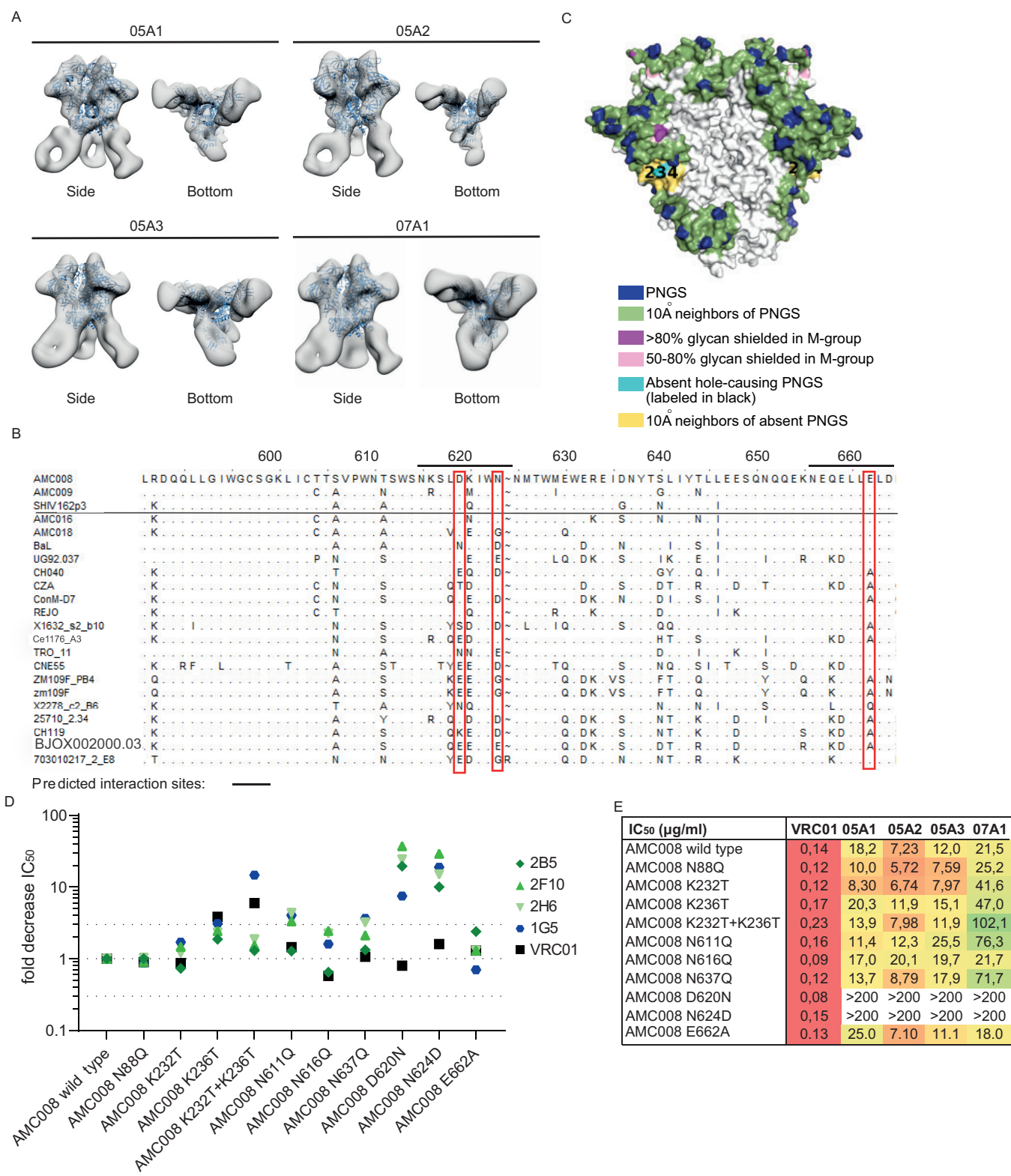


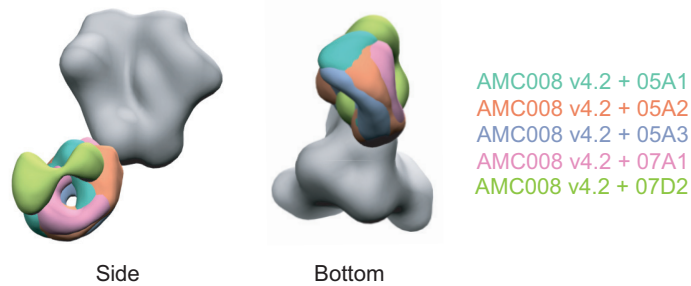
Fig 4

A

Ab ID	Fold change AUC											linear V3 peptide	
	AMC008 v4.2	AMC008 gp120	K232T	K236T	K232T+K236T	N88Q	N611Q	N616Q	N637Q	D620N	N624D		E662A
2G12	1.0	1.0	0.9	0.9	0.9	0.8	0.8	0.9	0.9	0.9	0.8	0.9	No
PGT145	1.0	ND	1.0	1.0	0.9	0.8	0.8	0.9	0.8	1.5	0.9	1.1	ND
05A1	1.0	0.1	0.8	0.7	0.7	0.8	0.8	0.8	0.9	0.7	0.6	0.8	No
05A2	1.0	0.1	0.9	0.9	0.9	0.3	0.8	0.9	0.9	0.9	1.0	1.0	No
05A3	1.0	0.1	0.9	0.9	1.0	0.9	1.0	1.0	0.9	1.0	0.8	0.9	No
05B1	1.0	ND	ND	ND	ND	ND	ND	ND	ND	1.0	1.0	1.0	ND
05B2	1.0	0.1	0.9	0.9	0.9	0.9	1.1	1.0	1.7	0.7	0.8	1.1	No
05D1	1.0	0.1	0.9	0.8	1.0	0.8	0.5	0.8	0.8	0.8	0.7	0.9	Yes
05G1	1.0	0.0	0.9	0.9	0.9	0.9	0.8	0.9	0.7	0.6	0.4	0.9	ND
06A1	1.0	0.0	0.8	0.8	0.8	0.9	0.5	0.8	1.0	1.0	0.8	1.0	ND
07A1	1.0	0.0	0.9	0.9	0.9	0.9	0.9	0.9	0.9	0.1	0.6	1.0	ND
07B1	1.0	1.4	1.0	1.0	1.0	1.0	1.0	1.1	1.0	0.9	1.0	1.2	No
07C1	1.0	0.1	1.0	0.9	1.0	0.9	1.1	1.1	1.1	0.7	0.9	1.1	No
07D1	1.0	ND	ND	ND	ND	ND	ND	ND	ND	ND	ND	ND	ND
07D2	1.0	0.0	1.0	0.7	0.7	0.7	0.6	1.2	1.2	0.1	0.1	0.1	ND
07E1	1.0	0.1	1.2	0.8	1.0	0.8	1.4	1.7	0.9	0.8	0.4	0.6	ND
07F1	1.0	0.1	1.0	1.0	0.8	0.9	1.0	1.0	0.3	0.9	0.9	0.9	No
07G1	1.0	ND	ND	ND	ND	ND	ND	ND	ND	ND	ND	ND	ND
08A1	1.0	ND	0.9	1.0	1.0	0.9	0.7	0.9	0.7	1.0	0.8	0.9	ND
			Strain specific glycan hole			gp41 glycans			NAb Interaction site			V3	

0.1-0.3
0.4-0.6
0.7-1.0
>1.0

B



A Fig 5

Neutralizing mAbs							
AMC008 SOSIP Env				AMC016 SOSIP Env			
Sample ID	KD (nM)	Ka (1/Ms)	Kd (1/Ms)	Sample ID	KD (nM)	Ka (1/Ms)	Kd (1/Ms)
05A1	7.74	1.57E+04	1.21E-04	05A1	7.58	2.39E+04	1.81E-04
05A2	12.0	2.23E+04	2.69E-04	05A2	3.91	3.36E+04	1.31E-04
05A3	10.0	1.07E+04	1.74E-04	05A3	18.0	1.74E+04	3.19E-04
07A1	8.35	1.83E+04	1.53E-04	07A1	7.65	2.61E+04	2.00E-04

Non-neutralizing mAbs							
AMC008 SOSIP Env							
Sample ID	KD (nM)	Ka (1/Ms)	Kd (1/Ms)				
05D1	1.95	9.72E+04	1.90E-04				
07D2	1.75	1.16E+05	2.03E-04				
07E1	0.7	1.15E+05	8.04E-05				

B

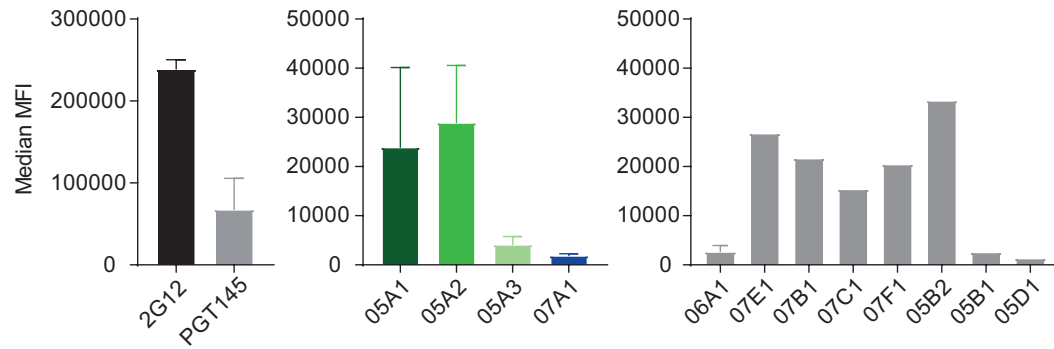
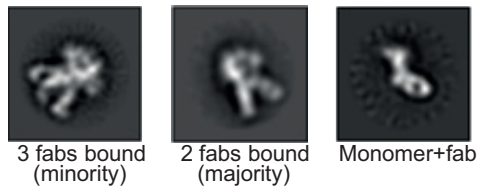


Fig 6

A



B

**AMC008 autologous virus**

Fold change IC <sub>50</sub>								
Time (h)	05A1	05A2	05A3	07A1	06A1	3BC315	PGT126	
1	1.0	1.0	1.0	1.0	NN	1.0	1.0	
3	1.2	1.5	1.5	1.6	NN	1.9	0.8	
6	1.9	2.3	2.1	2.4	NN	2.4	0.9	
24	12.4	7.9	10.2	11.4	NN	9.6	1.5	

**SHIV162p3 heterologous virus**

Fold change IC <sub>50</sub>							
Time (h)	05A1	05A2	05A3	07A1	3BC315	PGT126	
1	1.0	1.0	1.0	1.0	1.0	1.0	
3	1.7	4.8	3.6	11.5	9.1	0.5	
6	2.3	6.8	6.2	12.5	11.3	1.5	
24	4.8	18.5	15.9	28.1	21.4	4.5	



**Table 1:** Heterologous binding ability of the isolated NABs. (A) ELISA cross-binding ability (EC50 in  $\mu\text{g/ml}$ ) of the isolated AMC008 SOSIP trimer-reactive NABs to various clade B and non-clade B SOSIP Env trimers.

	Antibody ID	Clade	Tier	05A1	05A2	05A3	07A1
Clade B SOSIPs	AMC008	B	1B	++	++	++	++
	AMC009	B	2	++	++	++	++
	AMC011	B	2	-	-	+/-	-
	AMC016	B	3	++	++	++	+
	AMC018	B	2	++	++	++	+
	SHIV162p3	B	2	++	+	++	+/-
	REJO	B	2	++	++	++	++
non- clade B SOSIPs	BG505	A	2	-	-	-	-
	ConM	M	1A/1B	-	-	-	-
	CNE55	CRF01_AE	2	-	-	-	-
	BJOX002000.03.2	CRF07_BC	2	-	-	-	-
	Ce1176_A3	C	2	++	++	++	-
	HIV_25710-2.43	C	2	-	-	-	-

**Table 2:** Neutralization ability (IC50 in  $\mu\text{g/ml}$ ) of the autologous NABs to neutralize a panel of 17 heterologous viruses.

IC <sub>50</sub> ( $\mu\text{g/ml}$ )	Clade	Glycan hole	05A1	05A2	05A3	07A1	05D1
AMC008	B	230 + 234	20,5	14	15,1	16,2	>50
SHIV162p3	B	230	8,8	5,6	18	6,1	0,72
AMC009	B	230	177	58	170	114	>200
AMC016	B	-	>200	>200	>200	>200	>200
AMC018	B	234	>200	>200	>200	>200	>200
BaL	B	230 + 234	>200	>200	>200	>200	>200
WITO4160.33	B	234	>200	>200	>200	>200	>200
CH040	B	230 + 234	>200	>200	>200	>200	>200
CZA97.012	C	234	>200	>200	>200	>200	>200
ZM109F	C	234	>200	>200	>200	>200	>200
25710-2.43	C	230	>200	>200	>200	>200	>200
Ce1176_A3	C	-	>200	>200	>200	>200	>200
X2278	B	230	>200	>200	>200	>200	>200
BJOX002000.03.2	CRF07_BC	230	>200	>200	>200	>200	>200
Ce703010217_B6	C	-	>200	>200	>200	>200	>200
X1632-S2-B10	G	230	>200	>200	>200	>200	>200
CNE55	CRF01_AE	230	>200	>200	>200	>200	>200
CH119.10	CRF07_BC	230	>200	>200	>200	>200	>200